RANDOM TIME RESPONSE STATISTICS OF AVALANCHE PHOTODIODES AND ITS DEPENDENCE ON THE MEAN GAIN AND THE IMPACT IONIZATION RATIO

Thesis

Submitted to

Graduate Engineering and Research

School of Engineering

University of Dayton

In Partial Fulfilment of the Requirements for

The Degree

Master of Science in Electro-Optics

By

Guoquan Dong

University of Dayton

Dayton, Ohio

December 1998

RANDOM TIME RESPONSE STATISTICS OF AVALANCHE PHOTODIODES AND ITS DEPENDENCE ON THE MEAN GAIN AND THE IMPACT IONIZATION RATIO

APPROVED BY:

ABSTRACT

RANDOM TIME RESPONSE STATISTICS OF AVALANCHE PHOTODIODES AND ITS DEPENDENCE ON THE MEAN GAIN AND THE IMPACT IONIZATION RATIO

Name: Guoquan Dong
University of Dayton, 1998

Advisor: Dr. Majeed M. Hayat

The basic properties of avalanche photodiodes (APD's) and previous work related to the statistics of the APD random response time are first briefly reviewed. Following the detailed discussion of the avalanche multiplication processes in the multiplication region of APD's, the probability density function of the avalanche-limited random response time of APD's is characterized using renewal equations. The statistics of the random response time are then numerically computed from the renewal equations by using Picard iterations, and the dependence of the statistics of the random response time on the mean gain and the impact ionization ratio is investigated. It is found that the probability density function of the random response time decays exponentially. This thesis provides a new method to completely calculate the statistics of APD random response time, avoiding the complex numerically computation of the transport equations used by conventional methods.

To investigate the asymptotic behaviour of the probability density function of the random response time, the decay rates of the probability density function of the random response time, as functions of mean gain and the impact ionization ratio, are analytically determined. The basic assumption for the analytical solution is that the distribution functions of both hole and electron converge to unity exponentially. Comparison of the results shows that the exact numerical results are in good agreement with the analytical approximate solutions. Meanwhile, the analytical solutions to the decay rate show that the decay rate decreases as the mean APD gain increases, and decreases nearly exponentially as the impact ionization ratio increases.

The model developed in this thesis will facilitate developing simple approximate expressions for the receiver photocurrent. Two simple impulse response function models for the APD are proposed, and the analytical equations to calculate the statistics of the impulse response functions are derived in terms of the probability density function of the random response time. Finally, the possibility of extending the analysis to more complex models (e.g. incorporating the dead space effect and the non-uniform ionization coefficients) are discussed.

ACKNOWLEDGMENTS

I would like to express my sincerely appreciation to my advisor, Dr. Majeed M. Hayat, who assist me as research assistant during the summer, and ignite my research interest in this field. He is always willing to answer my question patiently and share his hand-on experience with me without any hesitation. Dr. Perry P. Yaney and Dr. Leno Pedrotti, the other members in my advisory committee. Both of who reviewed my thesis with dedication. They patiently read the paper, and correct technique and grammar errors. I really appreciate their comments and suggestions proved invaluable. Also, I would like to express my thanks to Mr. Torres Sergio Neftali, a graduate student in electrical engineering department, for many helpful suggestions. His initial algorithm on the Picard iteration method save me a lot of time.

Specially thanks due to Dayton Area Graduate Institute Scholarship (DAGIS) for providing me the full support to study here at University of Dayton, Electro-optics graduate program. Without this support, nothing could come to true.

Biggest thanks of all go to my wife Runjun Mao, for her constant support, encouragement, sacrifice and understanding, and also to my daughter, Sharlene Dong, for many weekends, I failed my promise to play with her. Without their love, none of this would have been possible.

TABLE OF CONTENTS

ABSTRACT iii

ACKNOWLEDGMENTS v

LIST OF ILLUSTRATIONS viii

LIST OF TABLES xi

CHAPTER

I. INTRODUCTION 1

1.1 Principal of operation of APD's 4

1.2 APD excess noise factor 7

1.3 Response speed.....8

1.4 APD noise currents 10

II. APD RANDOM RESPONSE TIME MODEL 12

2.1 Multiplication processes 12

2.2 Renewal theory for the random response time 16

2.3 Numerical solutions of the renewal equations.....21

2.4 Results and discussion 22

III. EXPONENTIAL TAIL OF THE PROBABILITY DENSITY FUNCTION OF THE RESPONSE TIME.....36

3.1 Analytical approximation to the Exponential tail of the probability density function of the response time..... 36

3.2 Analytical results and discussion 39

3.3 Comparision with the numerical results.....41

IV. APPLICATIONS 43

4.1 Impulse response function 44

4.2 Statistics of the impulse response function..... 46

4.3 Signal to noise ratio of the impulse response functio..... ..47

V. CONCLUSIONS ..... .49

REFERENCES.....52

LIST OF ILLUSTRATIONS

1.1. An APD together with the electric-field distribution inside various layers under reverse bias 6

1.2. Mean gain and the impact ionization ratio scatter diagram for different types of APD's 6

1.3. Simplified equivalent circuit diagram of an avalanche photodiode 9

2.1. Avalanche Photodiode Device Structure 13

2.2. Avalanche Processes when only electrons can impact ionize.... 14

2.3. Avalanche Processes when both holes and electrons contribute in the impact ionizing 15

2.4. APD multiplication process with the electron and hole current responses.....17

2.5. Multiplication process in the multiplication region, an electron at x initiates the multiplication process producing two offspring electrons and one hole at location x+ζ 19

2.6. Picard iteration procedure 23

2.7. Probability distribution functions as a function of normalized time for single carrier multiplication APD (k=0). The distribution function starts at electron transition time, and terminates at 2 times the transition time.....26

2.8(a). Probability distribution function of the random response time T as a function of the mormalized time t, for an APD with $v_e=v_h$. (a) The value of αw is chosen so that the mean gain is 10. The ionization coefficient ratio is set to 0.1,0.5 and 1.0 27

2.8(b).The value of αw is chosen so that the mean gain is 20. The ionization coefficient ratio is set to 0.1, 0.5 and 1.0 28

2.8(c).The value of αw is chosen so that the mean gain is 40. The ionization coefficient ratio is set to 0.1, 0.5 and 1.0 29

2.9(a). Probability density function of the random response time T as a function of the mormalized time t, for an APD with $v_e=v_h$. (a).The value of αw is chosen so that the mean gain is 10. The ionization coefficient ratio is set to 0.1,0.5 and 1.0 30

2.9(b). The value of αw is chosen so that the mean gain is 20. The ionization coefficient ratio is set to 0.1, 0.5 and 1.0 31

2.9(c). The value of αw is chosen so that the mean gain is 40. The ionization coefficient ratio is set to 0.1, 0.5 and 1.0 32

2.10. Mean of the response time <T> as a function of impact ionization coefficient ratio for means gain of 10, 20, and 40 33

2.11. Variance of the response time Var(T) as a function of impact ionization coefficient ratio for mean gain of 10, 20, and 40 34

3.1. Analytical decay rate of the pdf of the random response time T as a function of mean gain for fixed ionization coefficient ratio k.....40

3.2. Analytical decay rate of the pdf of the random response time T

as a function of mean gain for fixed ionization coefficient ratio k 41

3.3. Comparison result between the numerical and analytical decay rate γ

of the probability density function of the random response time T 42

4.1. Rectangular response model 43

4.3. Triangular response model 43

LIST OF TABLES

1.1. Characteristics of common APD's 7

2.1. The parameter αw used in the computation of the response times for various combinations of <G> and k. 24

CHAPTER I

INTRODUCTION

The demand for gigabit-rate fiber-optic communication systems and the rising popularity of the fiber optical links in RF/microwave systems have led to many advances in high-speed photodetector technology. Specific application requirements have spurred the development of novel device structures to improve the speed, responsivity, and the power handling capabilities of high speed detectors. Simultaneously, advances in materials and processing techniques have made these developments possible. In recent years there has been a renewed interest and widespread research effort in developing avalanche photodiodes (APD's). The driving force for this activity has been the development of new lightwave communication systems exploiting the low-loss and low-dispersion spectral windows at 1.3 and 1.55 μm of silica optical fibers [1-5]. Moreover, APD receivers exhibit higher sensitivity than PIN photodiodes due to the internal gain provided by APD's.

Conventional InGaAs APD's have a limited gain-band width product and a poor noise figure because of the small difference of impact ionization coefficient ratio in IV-V semiconductors used to fabricate these detectors [6,7]. Silicon APD's are well known for low multiplication noise and high gain-bandwidth product due to the large difference of hole and electron ionization coefficients [8]. However, the quantum efficiency of silicon

APD's is negligible at 1.3-1.55 μm, making them unusable for fiber communication systems. To enhance the gain and speed, and to obtain high gain-bandwidth product and high quantum efficiency, various novel APD structures have been proposed [9-16]. These include separate absorption, graded charge, and multiplication (SAGCM) structures [9-11], and more recently the resonant-cavity-enhanced photodiodes (RCE) have been realized as avalanche photodiodes [12-17].

With the development of the sophisticated structures and materials, there is an increasing need to develop better modeling techniques that can analyze the device performance and predict correctly and quickly the important operating parameters of the device. One of the important parameters of the device is the maximum bit rate at which it can operate. The response time greatly affects the maximum bit rate due to intersymbol interference (ISI) (resulting from the residual current due to the previous pulse). This effect is particularly important in avalanche photodetectors where the processes of avalanche multiplication have an inherent finite response time. For prediction of the maximum bit rate of an APD together with the overall performance of the receiver allowable, an accurate model for the APD time response is required. As we will discuss later, the multiplication process involved in the multiplication region of the APD is a random process. The statistical properties of the APD, such as the mean gain, the excess noise factor, and the probability density function (pdf) of the gain and the impulse response function are therefore very important in designing high data rate communication systems. Among these properties, the statistical properties of the impulse response

function of the APD play a crucial role in estimating the performance of such high data rate systems [18-20].

In this introductory chapter, the basic operation of APD's is briefly examined. The avalanche multiplication process will then be discussed in detail in the Chapter II. We will discuss the multiplication process separately for two reasons: First, this is the fundamental process, which completely determines the statistics of the gain and time response of an APD, and second, whatever the device structure is, the multiplication process is basically the same. The previous studies on the statistics of the impulse response function of the APD are briefly reviewed in the Section 2.2. Based on the techniques from branching theory, a general mathematical model for computing the statistics of the random response time is presented in the form of renewal integral equations. In contrast to the traditional methods of computing the mean, standard deviation and correlation of the APD impulse response function [17,18, 21-25], our method provides a simple way to compute the pdf of the random response time. After finding the pdf of the random response time, the statistical quantities associated with random response time, such as the mean of the response time, and its variance, as well as statistics of the impulse response function can be found. It is known that the decay rate of the pdf of the random response time plays an important role in calculating its associated statistical quantities. However, accurately computing the decay rate numerically (exactly) for high gain and large ionization coefficients ratio is very difficult. Therefore, an approximation solution for the decay rate of the pdf of the random response time is developed in the chapter III, and the validity of the approximation is discussed.

As described above, from the pdf of the random response time, the mean, the variance, and the autocorrelation function of the impulse response function can be derived easily avoiding the complex numerical solutions of the transport equations. This topic is addressed in the Chapter IV. Also, the signal-to-noise ratio for specific simple impulse response function model, together with the potential of further application of our theory are discussed. Finally, the main results of this thesis and comments on their significance are summarized in the Chapter V.

1.1 Principle of operation of an APD

Unlike conventional P-N or P-I-N photodiodes that generate a single electron-hole pair in response to the absorption of a photon, an APD can generate many electron-hole pairs from a single absorbed photon. This gain characteristic of the APD is due to the multiplication processes in the multiplication region (Figure 1.1)[26-32]. This internal gain makes APD's attractive for use in constructing sensitive receivers. Impact ionization is the basic parameter for multiplication of electrons and holes in high electric fields. The probabilities that an electron and a hole will have an ionizing collision in a distance dx are αdx and βdx, respectively, where α and β are the impact ionization coefficients for the electron and hole. For the carriers to obtain sufficient energy, the avalanche process requires a high bias voltage in order to generate a high electric field in the multiplication region. For a given temperature, the impact ionization coefficients are exponentially dependent on the electric field and have the functional form given by [33],

$$\alpha = a \exp\left(-\left(\frac{b}{E}\right)^{c}\right) \tag{1.1}$$

where *a, b* and *c* are experimentally determined constants, and *E* is the magnitude of the electric field in the multiplication region. Generally, this equation holds only over a limited range of the electric field due to the simplistic model on which it is based. Using Baraff's generalized

model [26], Okuto and Crowell developed a simple analytic expression for α and β that is valid over a wide range of electric fields [27],

$$\alpha = \left(\frac{eE}{E_i}\right)\exp\left(0.217\left(\frac{E_i}{E_r}\right)^{1.14} - \left\{\left[0.217\left(\frac{E_i}{E_r}\right)^{1.14}\right]^2 + \left(\frac{E_i}{eF\lambda}\right)^2\right\}^{\frac{1}{2}}\right) \tag{1.2}$$

in Eq.(1.2), E_i, E_r and λ are defined as the impact ionization threshold energy, the optical photon energy, and the mean free path for optical photon scattering, respectively, and *e* is the electron charge.

An important parameter for describing APD performance is the impact ionization ratio defined as,

$$k = \frac{\beta}{\alpha}$$

which is extensively used in the literature. From the application, the impact ionization coefficients, and therefore k, can be determined for different types of APD and different operating conditions using Eq.(1.2).

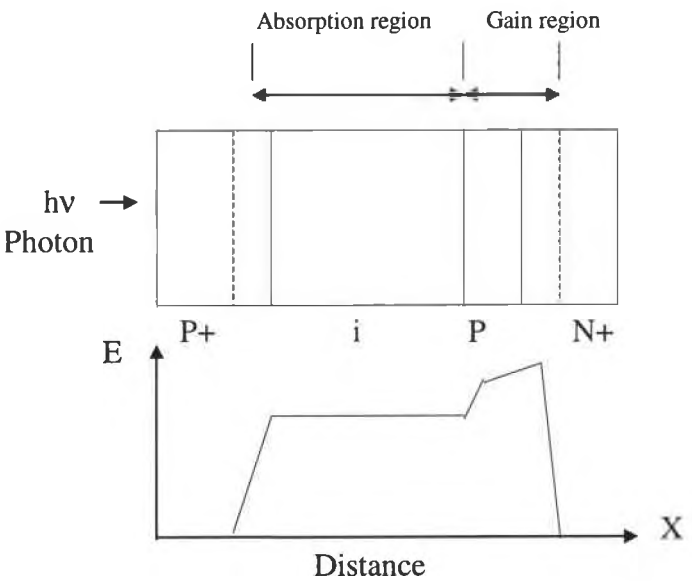

Figure 1.1. An APD together with the electric-field distribution inside various layers under reverse bias

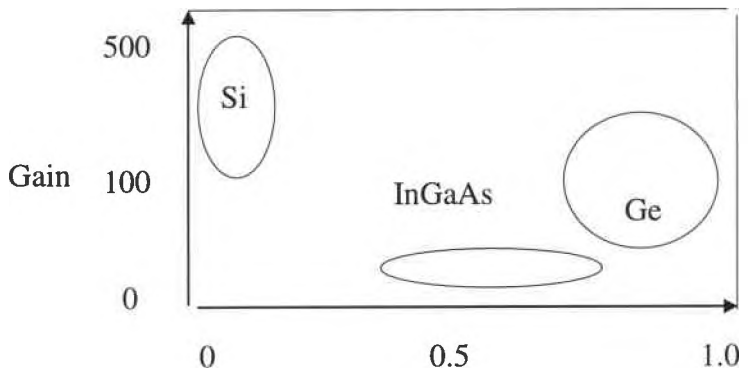

Figure 1.2. Mean gain and the impact ionization ratio scatter diagram for different types of APD's

1.2 APD excess noise factor

If the avalanche processes in the multiplication region were deterministic, in other words, if every injected photo carrier would produce the same gain G, the resulting noise would only be the multiplied input shot noise due to the random arrival of the signal photons. The avalanche processes is, instead, intrinsically statistical in nature so that individual carriers in general have different avalanche gains, characterized by a probability distribution. The excess noise factor then can be defined as [33,34],

$$F = \frac{<G^2>}{<G>^2} \qquad (1.3)$$

For typical silicon (Si) APD's, k ranges from 0.02-0.05, see table (1.1). For indium-gallium-arsenide (InGaAs) APD's, k ranges 0.5-0.7. As results, InGaAs APD are noisier than Si APD's. For germanium (Ge) APD's, k ranges 0.7-1.0, which means devices using Ge have higher noise level than devices obtained from such Si or InGaAs.

Table 1.1: Characteristics of common APD's (after [33,58])

Parameter	Unit	Si	Ge	InGaAs
Useful Wavelength Region	nm	400-1150	800-1750	900-1700
Responsivity (R)	A/W	80-130	3-30	5-20
Mean Gain Region	----	100-500	50-200	10-40
Impact Ionization Ratio (k)	----	.02-.05	0.7-1.0	0.5-0.7
Dark Current (I_d)	nA	0.1-1.0	50-1500	0.5-0.7
Rise Time (T_r)	ns	0.1-1.0	0.4-0.7	1-3
Bandwidth	GHz	0.2-1.0	0.4-0.7	1-3

1.3 Response speed

Typically, there are four time constants involved in determining the response speed of avalanche photodiodes: (1) The depletion-layer transit time τ_{tr}, (2) The RC time constant τ_{RC}, (3). The diffusion time in the undepleted layer τ_{D}, and (4) The avalanche build up time τ_{a}. The first three time constants strongly depend on the length of the depletion region.

The transit time can be simply obtained as [34,35],

$$\tau_{tr} = \frac{l_D}{v_s}$$

where l_D is the length of the depletion layer and v_s is the saturated drift velocity. l_D depends on structures, and v_s could be the saturated speed of an electron or hole.

The simplified equivalent circuit of an avalanche photodiode is given in the Figure 1.4. The RC response time is given by [35-38],

$$\tau_{RC} = (R_S + R_C)C$$

where R_s is the diode series resistance, R_c is the load resistance, and C is the diode capacitance, which is the sum of the junction and package capacitance. For carefully designed devices, a small value of 10-20 Ω can be typically obtained. The value of C is determined from the diode capacitance, which depends on the diode area, the length of the depletion layer and the package used.

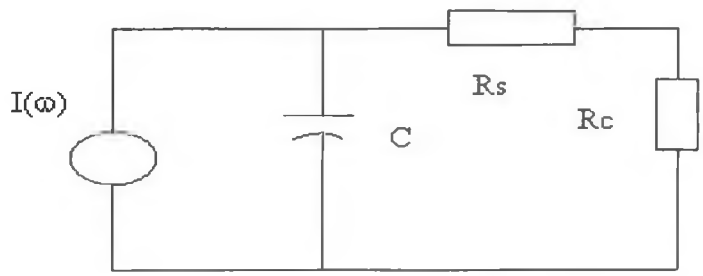

Figure 1.4 Simplified equivalent circuit diagram of an avalanche photodiode

The diffusion time in the undepleted layer τ_D has been shown to be [33,58],

$$\tau_D = \frac{l_0^2}{(2.4D)}$$

where l_0 is the distance of the carriers diffused in the undepleted region and D is the minority carrier diffusion constant. In well-designed devices, τ_D is usually much less than the other three time constants.

The multiplication process is not instantaneous. The avalanche build-up time τ_a depends on the number of secondary carrier generation and is sometimes roughly expressed proportional to the mean multiplication gain <*G*> as [31,33,34],

$$\tau_a = \langle G \rangle Nk\tau$$

where N is a number varying slowly from 1/3 to 2 and τ is the avalanche region transit time. This time constant depends strongly on the impact ionization coefficient ratio. If there is a large difference in these impact ionization coefficients, the time constant will be small.

Because the multiplication processes in the multiplication region is random. The multiplication buildup time is also a random variable. The above equations are only used to roughly estimate the buildup time. Therefore, in order to more accurately describe the performance of the device, it is necessary to examine the impulse response function of the detector, and to characterize the statistics of the impulse response function, such as the mean, the variance, and the autocorrelation function. This is the topic of many recent papers [51,53,59] that are discussed here in later sections.

Generally speaking, the APD response characteristics at high multiplication gain are governed by τ_a. On the other hand, the response speed at low multiplication gain is limited by the other factors. At low multiplication gain, there is a trade-off between the response speed and the quantum efficiency. This is due to the fact that the response speed is improved by reducing the absorption layer results in the decrease the quantum efficiency.

1.4 APD noise current

The total APD dark current consists of two components, I_{du} and I_{dm}. I_{du} is the unmultiplied current, which is mainly due to the surface leakage current, whereas I_{dm} is the bulk dark current experiencing the multiplication process. The total dark current can be expressed as

$$I_d = I_{du} + \langle G \rangle I_{dm} \tag{1.4}$$

By the definition of the excess noise factor F, the mean square noise current due to the dark current is given by

$$\left\langle I_d^2 \right\rangle = 2eI_{du} + 2eI_{dm}\langle G \rangle^2 F \tag{1.5}$$

From the previous discussion, we can see that the smaller the k, the smaller the excess noise factor. From the k values in the Table 1.1, we conclude that a Si APD has an excellent low dark current noise density compared with Ge APD and GaInAs/InP APD, which are usually used at longer (near infrared) wavelengths, whereas, Si APD's are used at short wavelengths.

In optical receiver applications, the photodetector is used with a low noise amplifier. The dark current noise power is given by,

$$\left\langle I_d^2 \right\rangle = 2eI_{du}BI_2 + 2eI_{dm}\langle G \rangle^2 FBI_2 \tag{1.6}$$

where B is the receiver bandwidth, and I_2 is an integral parameter which depends on the input optical pulse shape. This expression was first derived by Personic [35,36]. For rectangular input pulse that fill the bit time slot of duration $1/B$, and assuming a raised cosine output pulse, I_2 is about 0.55. More detailed information can be found in Personic's original work [35,36].

Equation (1.6) shows that the contribution of the unmultiplied dark currents to the output noise is generally negligible in comparison with the noise currents with multiplication. For example, at $<G>=20$, and $F \sim <G>^{1/2}$ (typical of $In_{0.53}Ga_{0.47}As$/InP APD's), the primary dark current is about 1 nA. After multiplication, it will reach to nearly 2 μA. Thus, for most practical receivers, we can ignore all unmultiplied noise sources of dark currents (e.g., detector surface currents, gate leakage, etc.) and consider only the current that undergoes multiplication.

CHAPTER II

APD RANDOM RESPONSE TIME

2.1 Impact ionization of carriers

The APD is a semiconductor device, which is normally operated in a strong reverse-biased manner in the p-n junction, which produce a depletion region of high electric field. Due to the thermal agitation and/or the presence of incident optical power, pairs of holes and electrons can be generated at various points within the diode (see Figure 2.1). These carriers drift toward opposite ends of the device under the influence of the applied electric field. When a carrier passes through the high-field depletion region. It gains sufficient energy to generate one or more new pairs of holes and electrons through a process called impact ionization in the depletion region. These new pairs can in turn generate additional pairs by the same mechanism. Carriers are collected at opposite ends of the diode. The likelihood that a carrier generates a new pair when passing through the high field region depends on the several factors, such as the type of carrier (hole or electron), the material of the region, and the reverse bias voltage. It can be assumed that impact ions produced are randomly located in the depletion region, and the numbers of ions are also randomly produced. Furthermore, we will neglect the space-charge effect. The gain and the response time associated with the random multiplication processes, are therefore also random variables.

Figure 2.2 illustrates the case when holes do not contribute to the impact ionization, (i.e.,k<<1). A parent electron that enters the multiplication region is rapidly accelerated by the strong applied electric field. A series of impact ionizations occur resulting in five electrons generated from a single parent photoelectron (G=5). Figure 2.3 shows the case when $k \approx 1.0$ where both electrons and holes contribute to the impact ionization. Electrons moving to the right can cause impact ionization to produce a new pair of electron and hole. Both electron and hole can generate additional pairs.

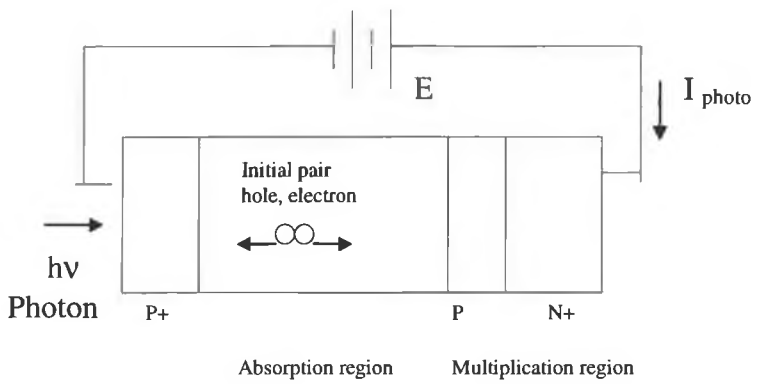

Figure 2.1 Avalanche photodiode device structure

The general features of the gain process can be seen in the Figure 2.2. The direction of the field is assumed to be as shown, so that electrons within the multiplication region travel in the positive x direction and holes travel in the negative x direction. Thus, the direction of current flow is in the same direction as the electric field.

The electron current increases with increasing x while the hole current decreases with increasing x.

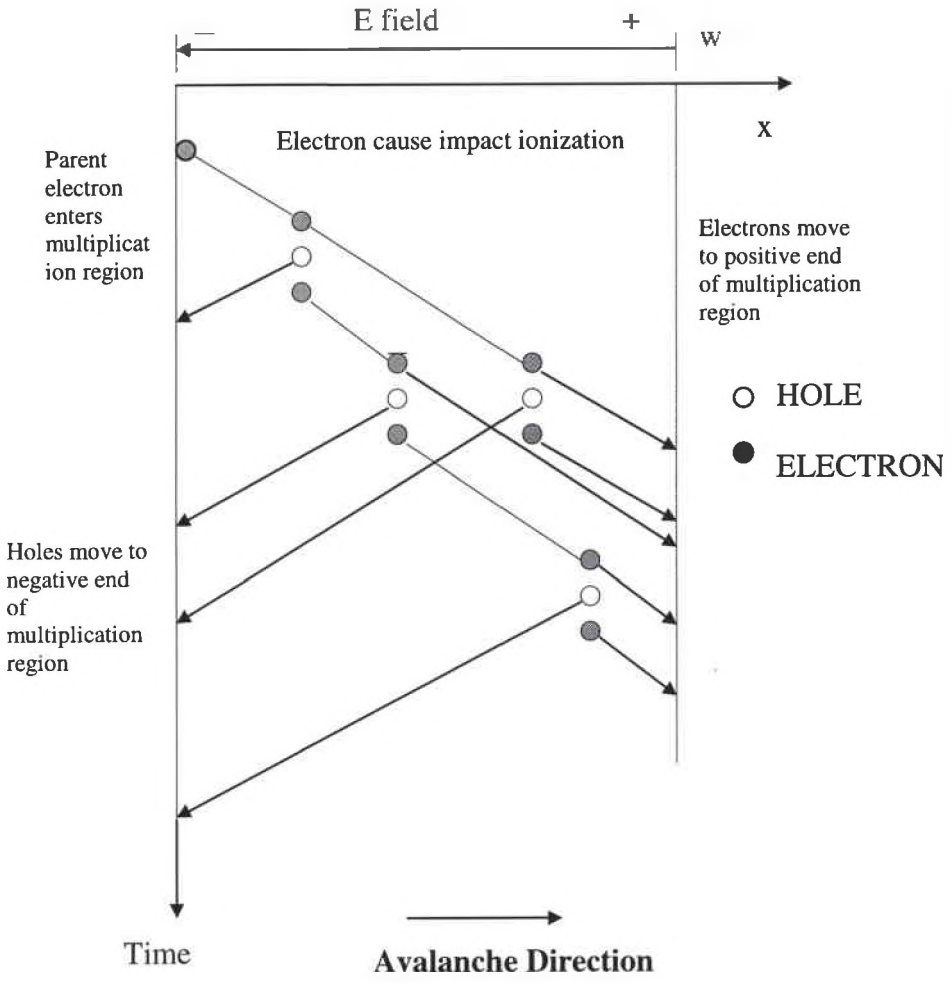

Figure 2.2 Avalanche processes when only electrons can impact ionize

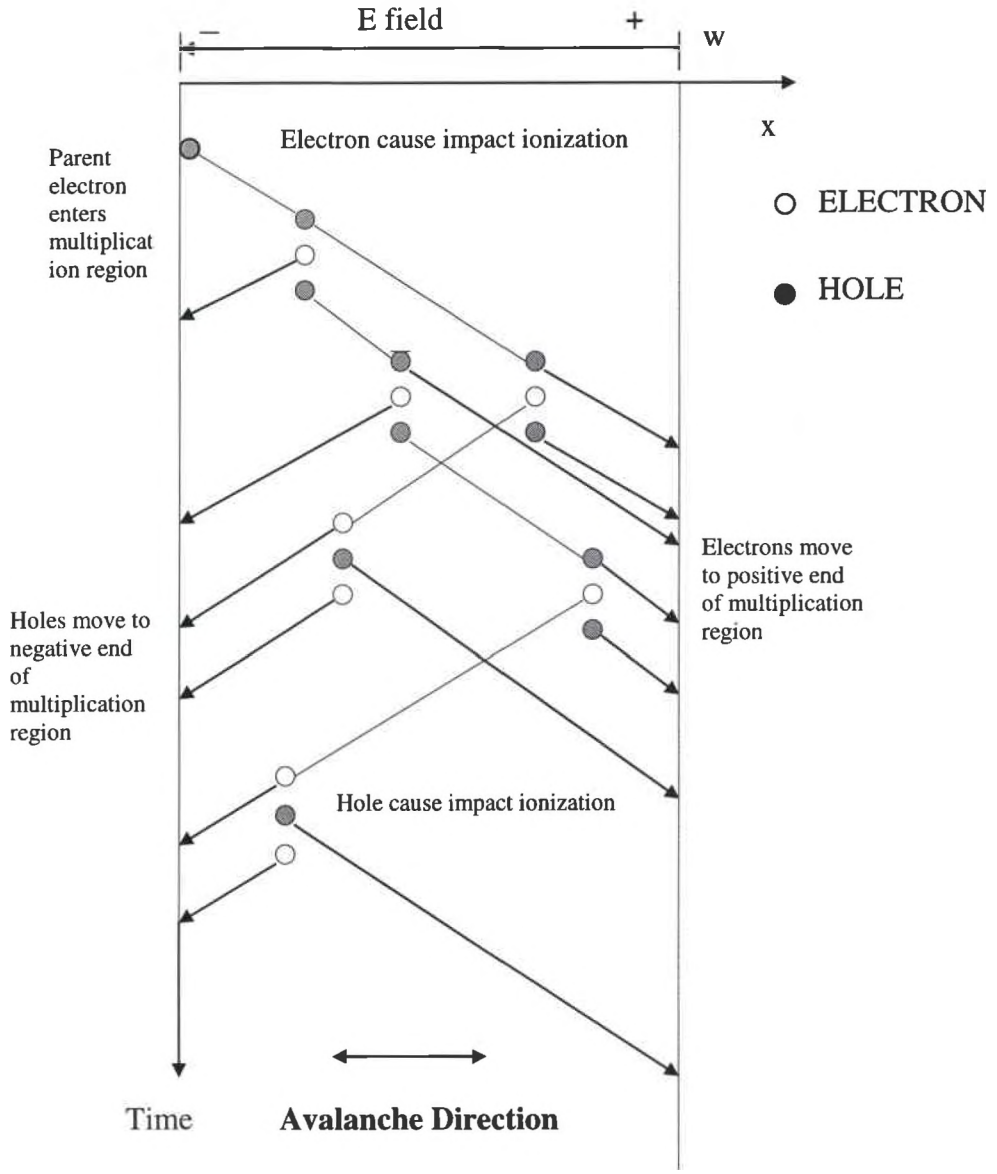

Figure 2.3 Avalanche processes when both holes and electrons contribute in the impact ionizing

2.2 Renewal theory for the random response time

In the Section 2.1, the focus is on the basis of the gain process. This process is a random process, and the gain statistics has been extensively studied [30,31,35,39-45]. However, most of the work does not address the time dependence of the avalanching process. In order to analyse the performance of digital optical communication systems, knowledge of the temporal statistics of the impulse response function is required. Studies of the temporal response of the APD were limited to the mean value, its variance, and its auto-correlation function. Nagvi [46] provided an expression for the mean square avalanche current by including a frequency dependent factor based on McIntyre's expression [28]. Naqvi solved the transport equations for the mean current densities assuming stationary multiplication process. Walma and Hackam [47] provided a partial solution of the problem by considering only the arrival of electrons at the edge of the device. They did not determine the photocurrent response. The autocorrelation function of the impulse response was first determined by Matsuo et al [48,49]. The statistics of the random response time, which is finite for each ionization of the impulse response, and the relation between the random response time and the statistics of the impulse response current is not clear [50-53]. However, direct knowledge of the mean, variance, and the probability density function of the APD response time can be effectively used to obtain simple approximate expression for the statistics of the receiver photocurrent. In this chapter, the pdf of the random response time of APD's is characterized using renewal equations. The pdf, and therefore the statistics of the response time are then numerically

computed from the renewal equations. Simple approximations for the statistics of the receiver impulse response function based on the pdf of the random response time will be discussed in the chapter IV.

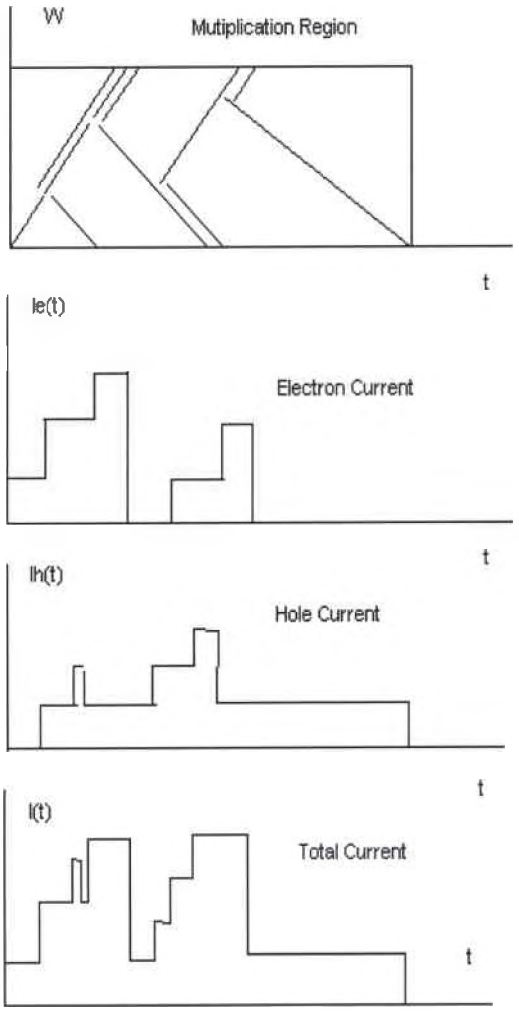

Figure 2.4: APD multiplication process with the electron and hole current responses

Consider the multiplication region in the APD as shown in Figure 2.4 and 2.5, define *I(t)* as the photocurrent in the multiplication region. The random response time T is the time it takes until all the carriers exit the multiplication region. In other words, it is the time it takes until the photocurrent goes to zero. Mathematically, it can be expressed as,

$$T = \min\{t: I(t) = 0\}$$

For single carrier multiplication devices, T is bounded by the sum of the electron and hole transit

times. That is,

$$T \leq \frac{w}{v_e} + \frac{w}{v_h}$$

But for the double carrier multiplication APD's, each realization of *I(t)* is of finite extent (assuming finite gain), but the duration of *I(t)* is random and cannot be bounded.

Let $F_T(t)=P\{T\leq t\}$ denote the probability distribution function (PDF) of the random response time T, and let $T_e(x)$ be the time when the APD response terminate if the multiplication is initiated by a single electron at location x, (see Figure 2.5). Finally, we let $F_e(t,x)=P\{T_e(x)\leq t\}$ be the PDF of the random variable $T_e(x)$. Clearly we have $F_T(t)=F_e(t,0)$. If the first electron ionization occurs at $x+\zeta$, then the response will die out only if the response resulting from the offspring two electrons and hole terminate. Since a parent electron at x must travel a distance w-x before exiting the multiplication region. Therefore, $F_e(t,x)=1$ for $t \geq (w-x)/v_e$, where v_e is the saturate velocity for electron. Similarly, the PDF for the random variable $T_h(x)$ can be expressed as $F_h(t,x)=P\{T_h(x)\leq$

t}, and a hole necessary travels a distance x before existing the multiplication region. $F_h(t,x)=1$ for $t > x/v_h$, where v_h is the saturation velocity for hole. Using the techniques from the branching theory [54-56], it can be shown that the distribution function $F_e(t,x)$ and $F_h(t,x)$ are related by the following renewal integral equations,

$$Fe(t,x) = [e^{-\alpha(w-x)} + \int_0^{w-x} F_e^2(t-\tfrac{\xi}{v_e}, x+\xi) F_h(t-\tfrac{\xi}{v_e}, x+\xi)\alpha e^{-\alpha\xi} d\xi]\, U(t-\tfrac{w-x}{v_e}) \qquad (2.1)$$

$$F_h(t,x) = [e^{-\beta x} + \int_0^{x} F_h^2(t-\tfrac{\xi}{v_h}, x-\xi) F_e(t-\tfrac{\xi}{v_h}, x-\xi)\beta e^{-\beta\xi} d\xi]\, U(t-\tfrac{x}{v_h}) \qquad (2.2)$$

where U(.) is the unit step function.

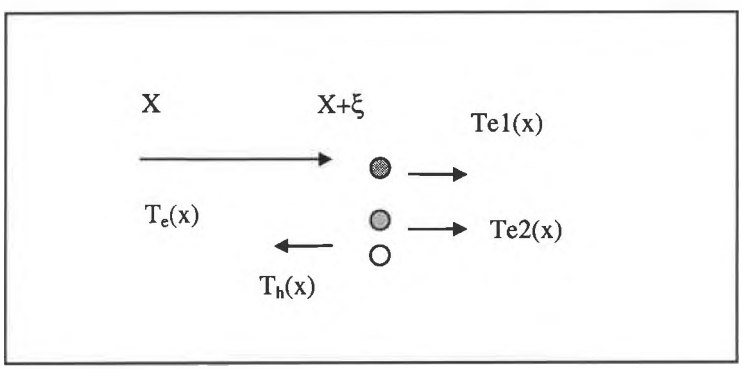

Figure 2.5: Multiplication process in the multiplication region, an electron at x initiates the multiplication process producing two offspring electrons and one hole at location x+ζ

To obtain Eq.(2.1) and (2.2), we first assume a parent electron at position x, then consider the condition on the location of its 1st ionization. If no ionizing take place, then

$$P\{T_e(x) \le t\} = \begin{cases} 1 & t > v_e/w-x \\ 0 & other \end{cases}$$

On the other hand, if the 1st ionization occurs at $\zeta \geq x$, then in order for $T_e(x)$ to be less than t, the response times $T_{e1}(\zeta)$, $T_{e2}(\zeta)$ and $T_h(\zeta)$, correspond to the offsprings at ζ must all expire within at time $t - (\zeta - x)/v_e$. By using the independence of $T_{e1}(\zeta)$, $T_{e2}(\zeta)$ and $T_h(\zeta)$, and averaging over all possible ζ in [x,w], we obtain (2.1).

In Equation (2.1), the first part of the right hand side is the probability that the parent electron at x is transported to the end of the multiplication region without ionizing. The integral represents the event that the parent electron impacts ionization during its travel from x to w. Similar interpretation is associated with hole in the Equation (2.2).

For the convenience of computation, we set,

$$X' = \frac{X}{w} \quad , \qquad \varsigma' = \frac{\varsigma}{w} \quad , \qquad \text{and} \qquad t' = \frac{t}{\tau_e}$$

where $\tau_e = w/v_e$, is the electron transit time through the multiplication region.

The purpose of changing variables is to normalize all variables to dimensionless quantities. After normalization, the renewal equations (2.1) and (2.2) can be rewritten as,

$$F_h(t,x) = [e^{-\beta wx} + \int_0^x F_h^2(t - \xi\tfrac{v_e}{v_h}, x-\xi) F_e(t - \xi\tfrac{v_e}{v_h}, x-\xi) h_h(\xi) d\xi]\, U(t-x) \qquad (2.3)$$

$$Fe(t,x) = [e^{-\alpha w(1-x)} + \int_0^{1-x} F_e^2(t-\xi, x+\xi) F_h(t-\xi, x+\xi) h_e(\xi) d\xi]\, U[t-(1-x)] \qquad (2.4)$$

where $h_e(\varsigma) = \alpha e^{-\alpha wx}$

$h_h(\varsigma) = \beta e^{-\beta wx}$

The distribution function $F_e(x,t)$ and $F_h(x,t)$ can be then numerically solved from renewal equations by using an iteration method. Finally, the distribution function for the response time can be found through the relation that,

$$F_T(t) = F_e(t,0)$$

2.3 Numerical solution of the renewal equations

The numerical solutions to the distribution function of $F_e(x,t)$ and $F_h(x,t)$ can be implemented using the Picard iteration method. It has been demonstrated [51,57] that Picard iteration method is a simple and efficient numerical recipe, although it may not be the best one. The general procedure is illustrated in the Figure (2.6). Initially, we set $F_e(t,x)$ and $F_h(t,x)$ both equal to 0 for any $t \in [0,1]$ and $x \in [0,1]$, then we start the iteration as follow.

Let us write the renewal equations as,

$$F_e(t,x) = L_e(F_e, F_h)(t,x)$$

$$F_h(t,x) = L_h(F_e, F_h)(t,x)$$

where L_e and L_h are operators that map two functions of two variables to a function of two variables. In our case, the operators are the exponential term plus integrals. The iterations can then be expressed as,

$$F_e^{n+1}(t,x) = L_e(F_e^n, F_h^n)(t,x)$$

$$F_h^{n+1}(t,x) = L_h(F_e^n, F_h^n)(t,x)$$

After the initial values are set, the iteration procedure can be continued until the pre-set convergence criterion is met. That is,

$$MAX\left[F_e^{n+1}(t,x) - F_e^n(t,x)\right] < \varepsilon$$

and $$MAX\left[F_h^{n+1}(t,x) - F_h^n(t,x)\right] < \varepsilon$$

where ε is the pre-set tolerance, and t∈ [0,1], x∈ [0,1].

It can be shown [56,57] using elementary analysis that the sequence of functions $\left\{F_e^n(t,x)\right\}_{n=0}^{\infty}$ and $\left\{F_h^n(t,x)\right\}_{n=0}^{\infty}$ is Cauchy in the supernum norm metric, hence there exist limit functions to which $F_e(t,x)$ and $F_h(t,x)$ convergence uniformly.

2.4 Results and Discussion

The renewal theory discussed in the Chapter 2 is applied generality to both a single carrier and a double carrier APD's. For simplicity, without lose of generosity, we assume that the saturation velocity of electrons and holes are the same, that is, $v_e = v_h$. In a real APD structure, many factors will affect the APD response time [58]. As we discussed in the chapter 2, in a well-designed device, the transit time effect and the avalanche build-up time will dominate. However, for a specific device, the transit time in the depletion layer is relatively unchanged, and also it is much less than avalanche build-up time for avalanche photodiode operating at high gain. For the above reason, only the effect of the avalanche build up time is considered in this thesis. In our computations of the PDF of the response time, the parameters given in

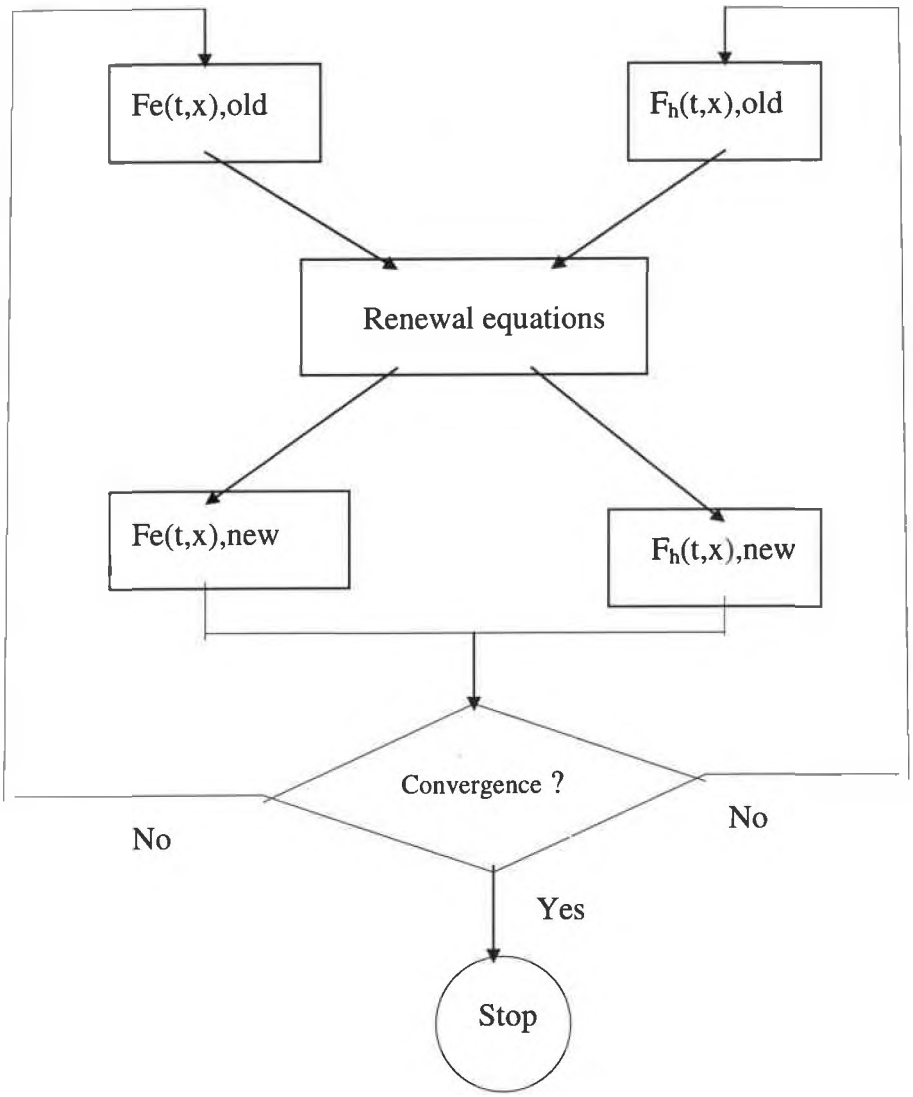

Figure 2.6 : Picard iteration procedure

Table 2.1: The parameter αw used in the computation of the response time for various combinations of Given <G> and k,

k	<G>=10 <G>=10	<G>=20	<G>=40
0.1	1.845	2.146	2.333
0.2	1.591	1.784	1.893
0.3	1.420	1.562	1.639
0.4	1.294	1.407	1.466
0.5	1.196	1.289	1.337
0.6	1.116	1.195	1.236
0.7	1.049	1.118	1.153
0.8	0.992	1.054	1.085
0.9	0.943	0.998	1.026

Table 2.1 are used. Given a mean gain and an ionization coefficient ratio k, α and k can then be computed [33].

Figure (2.7) shows the distribution function of random response time T for single carrier multiplication devices. As we pointed out in the previous section, for a single carrier multiplication devices, T is bounded by the sum of the electron and hole transit time. For the same electron and hole saturation speed, the response time T is less than $2\tau_e$. From Fig. (2.7), it is clear that the distribution function starts from a small value at τ_e, and increases rapidly to 1 at $T = 2\tau_e$. For the probability density function of a single carrier device, because the distribution function is discontinuous at $T = \tau_e$, the δ function

appears in the probability density function. Fig.(2.8a) shows the distribution function of T as a function of response time T for the different impact ionization ratios, k = 0.1, 0.5, 1.0 and for fixed mean gain <G> = 10. Fig.(2.8b) and (2.8c) are similar to (2.8a), except that for the mean gain is <G> = 20 and 40, respectively.

To analyze the tail of the distribution function of the random response time T in detail, we plotted the probability density function of T as a function of the time t in the Fig. (2.9a), (2.9b), and (2.9c). As shown in the Figures, for $T>5\tau_e$, the pdf of T is almost exponential. This observation serves as a basic assumption in the next Chapter to analytically compute the decay rate of the pdf of the random response time T. Figures (2.10) and (2.11) show the mean response time <T> and variance Var(T) as a function of the impact ionization ratio k for different mean gain. These results are in consistent with the results reported in the literature [51,53]. However, the theory developed in [51,53] is only suitable to calculate the statistics of the impulse response function, and not the statistics of the random response time itself. The statistics

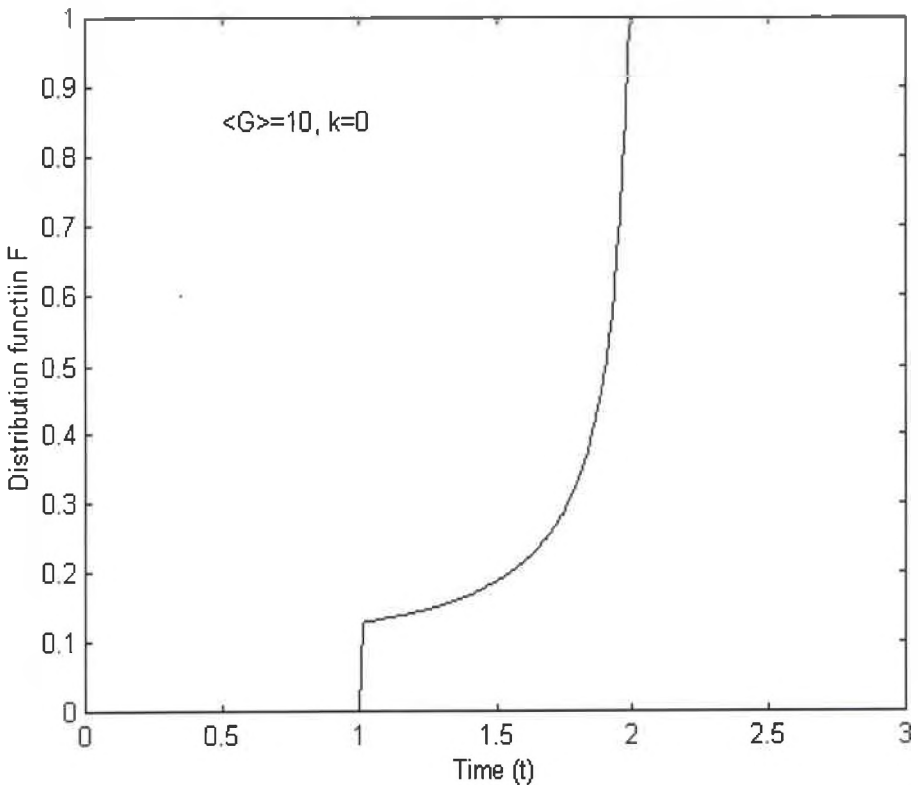

Figure 2.7. Probability distribution function as a function of normalized time for single carrier multiplication APD (k=0). The distribution function is zero prior to the transit time, and terminates at 2 times the transition time.

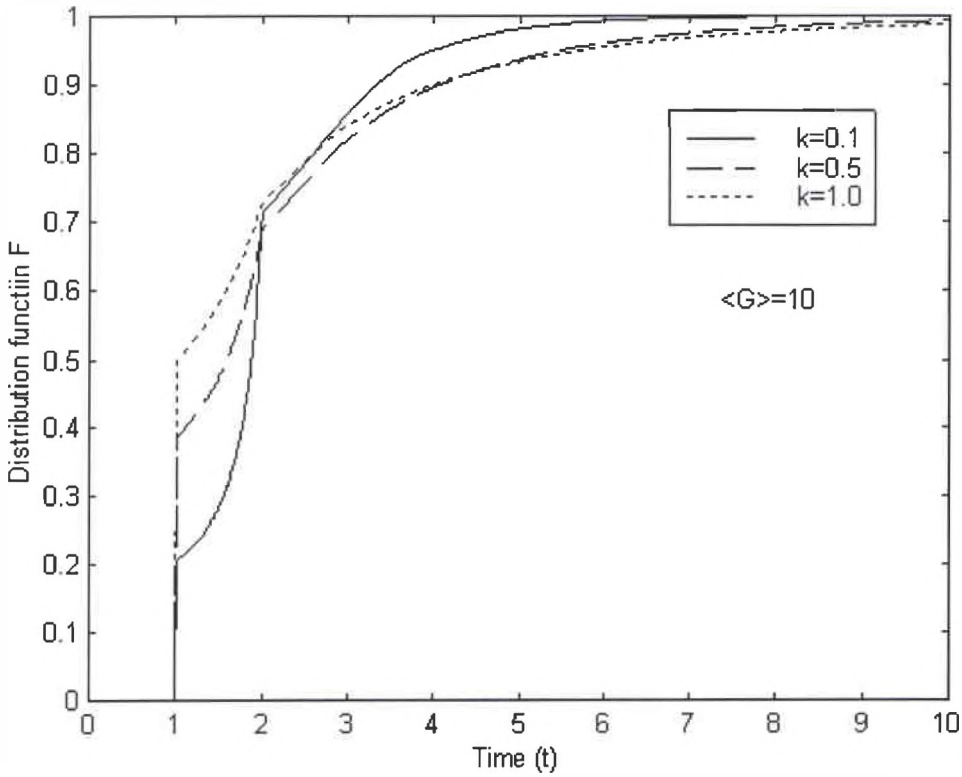

Figure 2.8. Probability distribution function of the random response time T as a function of the normalized time t, for an APD with $v_e = v_h$. (a) The value of αw is chosen so that the mean gain is 10. The ionization coefficient ratio is set to 0.1, 0.5 and 1.0

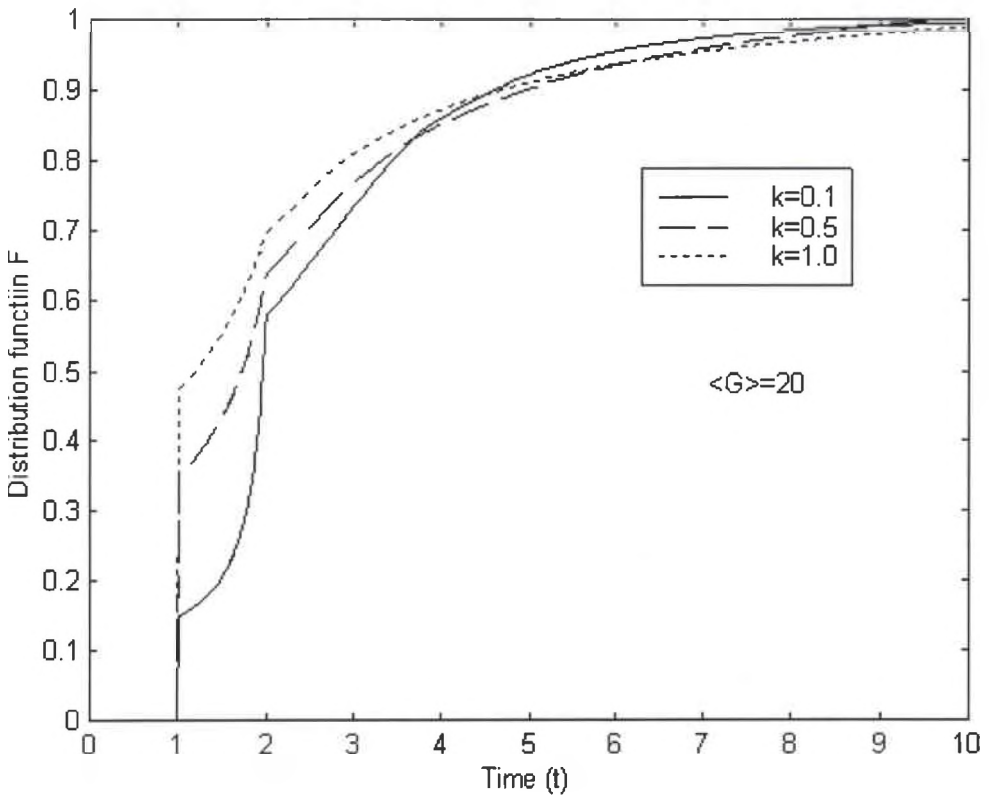

Figure 2.8 (b). The value of αw is chosen so that the mean gain is 20. The ionization coefficient ratio is set to 0.1, 0.5 and 1.0.

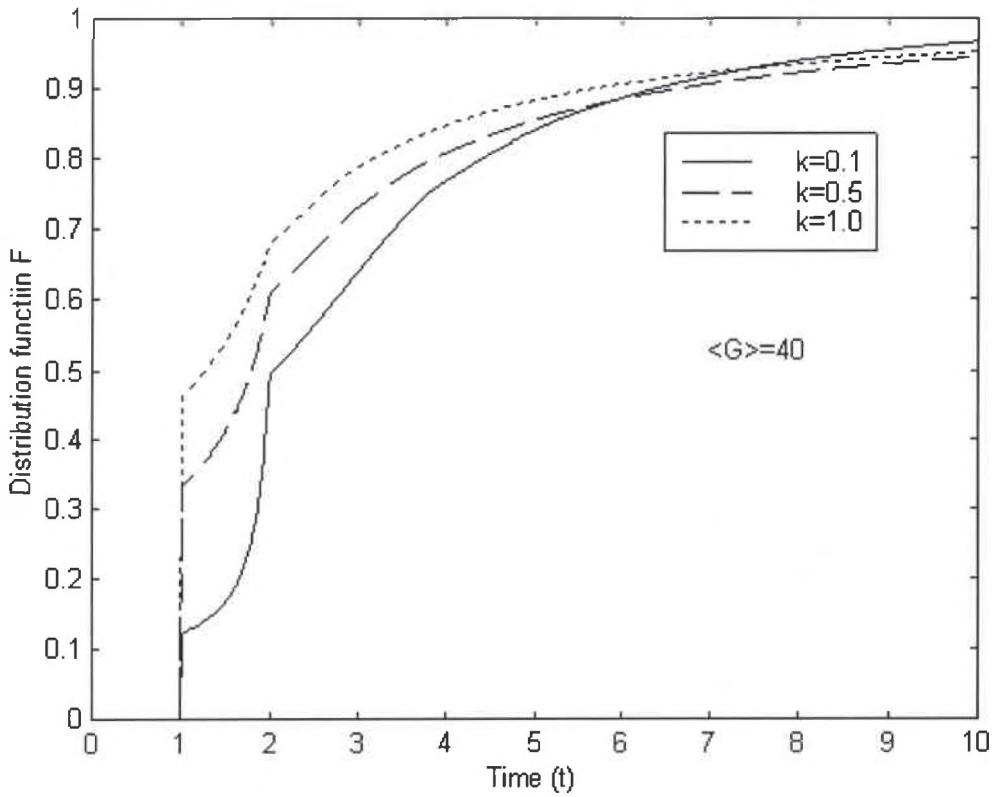

Figure 2.8 (c). The value of αw is chosen so that the mean gain is 40. The ionization coefficient ratio is set to 0.1, 0.5 and 1.0.

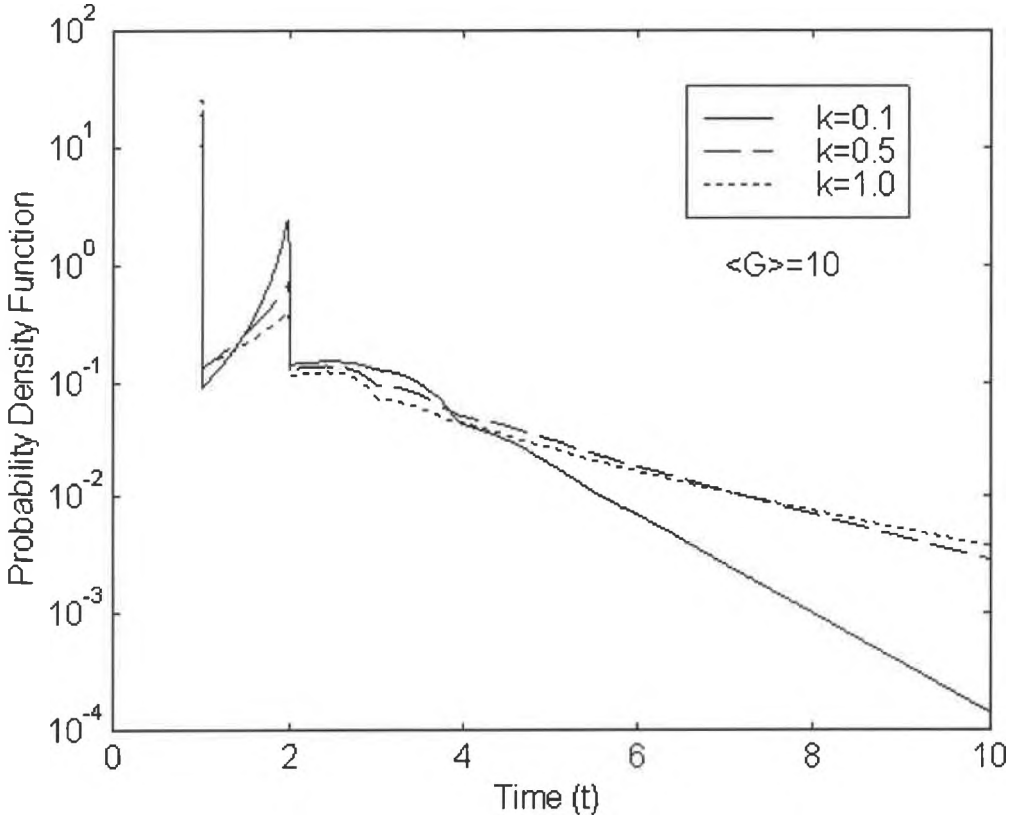

Figure 2.9 (a). Probability density function of the random response time T as a function of the normalized time t, for an APD with $v_e = v_h$. The value of αw is chosen so that the mean gain is 40. The ionization coefficient ratio is set to 0.1,0.5 and 1.0.

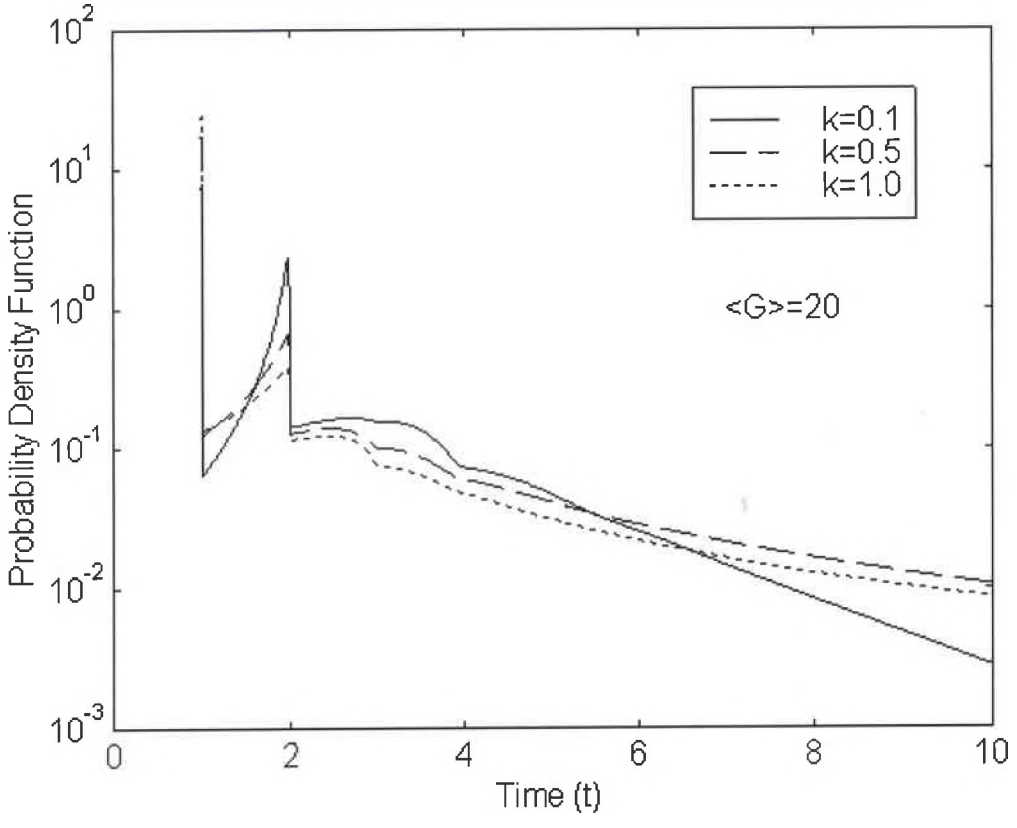

Figure 2.9 (b). The value of αw is chosen so that the mean gain is 20. The ionization coefficient ratio is set to 0.1, 0.5 and 1.0.

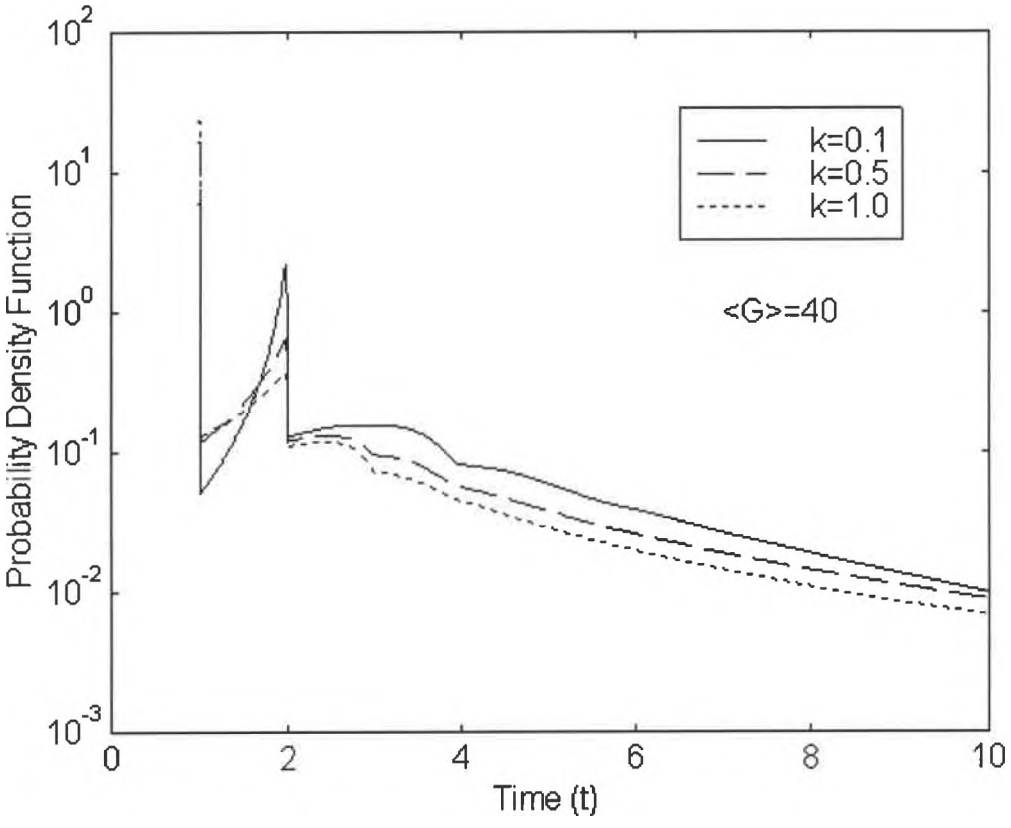

Figure 2.9 (c). The value of αw is chosen so that the mean gain is 40. The ionization coefficient ratio is set to 0.1, 0.5 and 1.0.

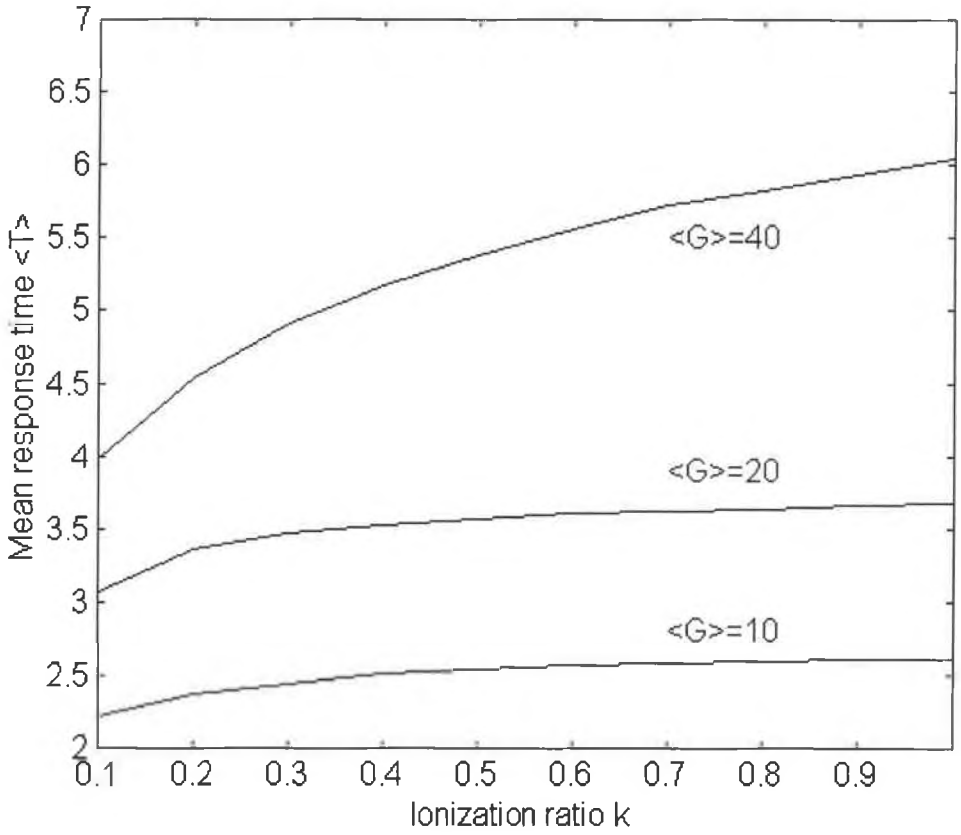

Figure 2.10. Mean of the response time <T> as a function of impact ionization coefficient ratio k for mean gain of 10, 20, and 40.

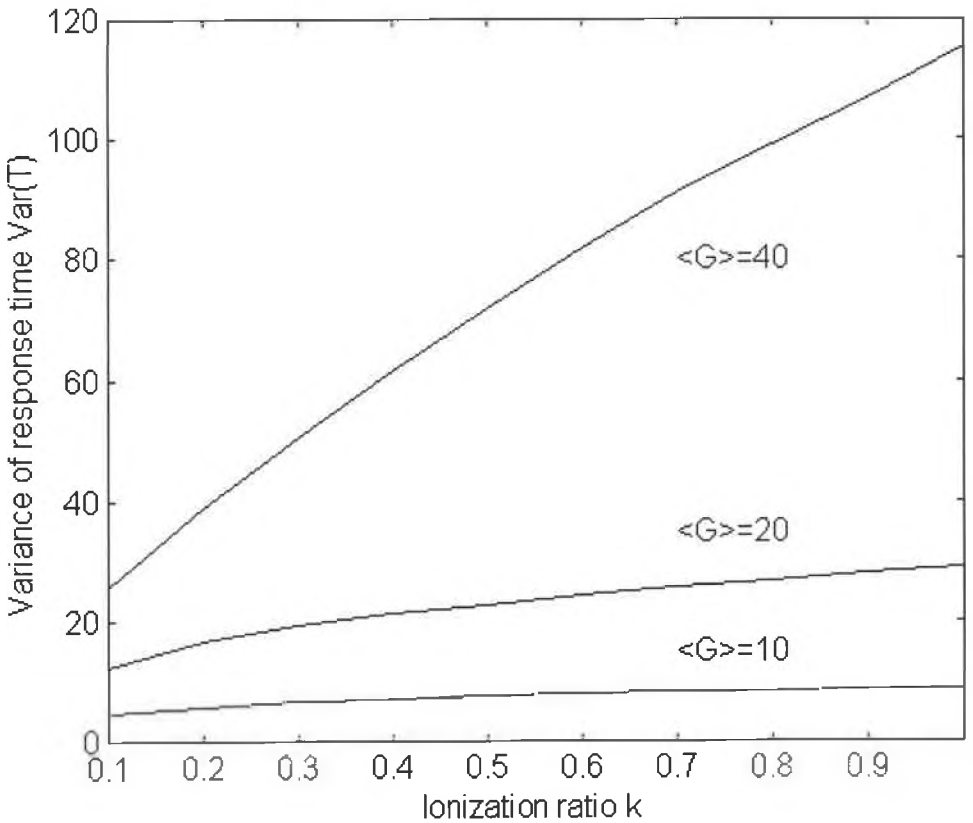

Figure 2.11. Variance of the response time Var(T) as a function of impact ionization coefficient ratio for mean gain of 10, 20, and 40.

of the random response time tells us exactly how the mean and variance of the random response time increase with the mean gain and the impact ionization ratio k. In Figures (2.14) and (2.15), it is shown that for high gain APD's, both the mean and the variance increase greatly. For high rate digital optical communication systems, these effects will increase the effect of intersymbol interference and therefore limit the bit-error-rate.

CHAPTER III

EXPONENTIAL TAIL OF THE PROBABILITY DENSITY FUNCTION OF THE RESPONSE TIME

3.1 Analytical approximation to the exponential tail of the probability density function of the response time

In Chapter II we observe that the PDF's of the electrons and holes, $F_e(t,x)$ and $F_h(t,x)$, respectively, converge to unity exponentially fast. Let the exponential rates for electron and hole be γ. The PDF of the electron and hole can then be assumed to be,

$$F_e(t,x) = 1 - A(x)\exp(-\gamma t) \qquad (3.1)$$

$$F_h(t,x) = 1 - B(x)\exp(-\gamma t) \qquad (3.2)$$

where A(x) and B(x) are constants with respect to time.

At the edge of the multiplication region, that is at $x = 1$, the PDF of $T_e(1)$ must be 1 whatever the time is, since $T_e(0)=0$. Therefore, $F_e(t,1)=1$. Similarly for hole, $F_h(t,0)=1$ at $x=0$. Inserting these two boundary conditions into equations (3.1) and (3.2), we obtain,

$A(1) = 0$

and $B(0) = 0$

Inserting equations (3.1) and (3.2) into the normalized master renewal equations, and neglecting the high order terms, we obtain,

$$A(x)=\int_0^{1-x}2\alpha A(x+\varsigma)\exp[(\gamma-\alpha)\varsigma]d\varsigma$$
$$+\alpha\int_0^{1-x}B(x+\varsigma)\exp[(\gamma-\alpha)\varsigma]d\varsigma \qquad (3.3)$$

Now use the change of the variable, $\eta = x+\xi$, obtain,

$$A(x)=\int_x^{1}2\alpha A(\eta)\exp[-(\gamma-\alpha)(\eta-x)]d\eta$$
$$+\alpha\int_x^{1}B(\eta)\exp[(\gamma-\alpha)(\eta-x)]d\eta \qquad (3.4)$$

By differentiating both sides of Equation (3.4) with respective to x, and applying the boundary conditions, we obtain,

$$A'(x)=-\alpha A(x)-\alpha B(x)-\gamma A(x) \qquad (3.5)$$

We can apply the same procedure and obtain,

$$B'(x)=\beta B(x)+\beta A(x)+\gamma B(x) \qquad (3.6)$$

For convenience, define the vector,

$$D(x)=\begin{bmatrix}A(x)\\B(x)\end{bmatrix}$$

Then Equation (3.5) and (3.6) can be expressed as,

$$D'(x)=MD(x) \qquad (3.7)$$

where the matrix M is given by,

$$M=\begin{bmatrix}-\gamma-\alpha & -\alpha\\ \beta & \beta+\gamma\end{bmatrix}$$

The differential equation (3.7) generally has solutions $A(x)$ and $B(x)$ of the following form,

$$A(x) = c_1 \exp(r_1 x) + c_2 \exp(r_2 x) \tag{3.8}$$

$$B(x) = d_1 \exp(r_1 x) + d_2 \exp(r_2 x) \tag{3.9}$$

By applying the boundary conditions to Equations (3.8) and (3.9), we obtain,

$$c_1 \exp(r_1) + c_2 \exp(r_2) = 0 \tag{3.10}$$

and $$d_1 + d_2 = 0\ , \tag{3.11}$$

By inserting the general solutions into equation (3.7), we obtain,

$$\begin{aligned} c_1 r_1 &= -2c_1\alpha - d_1\alpha - (\gamma - d)c_1 \\ c_2 r_2 &= -2c_2\alpha - d_2\alpha - (\gamma - \alpha)c_2 \end{aligned} \tag{3.12}$$

and

$$\begin{aligned} d_1 r_1 &= d_1\beta + c_1\beta + d_1\gamma \\ d_2 r_2 &= d_2\beta + c_2\beta + d_2\gamma \end{aligned} \tag{3.13}$$

From Equation (3.12) and (3.13), we derive the following linear equation in matrix form, and the

relationship between c_1 and c_2 is given by,

$$c_2 = -c_1 \frac{r_1 + \alpha + \gamma}{r_2 + \alpha + \gamma} \tag{3.14}$$

and

$$\begin{bmatrix} r_1 + \alpha + \gamma & \alpha \\ -\beta & r_1 - \beta - \gamma \end{bmatrix} \begin{bmatrix} c_1 \\ d_1 \end{bmatrix} = \begin{bmatrix} 0 \\ 0 \end{bmatrix} \tag{3.15}$$

The homogeneous linear equation (3.15) has a non-trivial solutions if and only if the determinant of the coefficients matrix is zero, that is,

$$\det\left(\begin{bmatrix} r_1+\alpha+\gamma & \alpha \\ -\beta & r_1-\beta-\gamma \end{bmatrix}\right)=0 \qquad (3.16)$$

This condition leads to the non-linear characteristic equation,

$$r^2+ r(\alpha+\beta)-\gamma (\alpha+\beta+\gamma) = 0 \qquad (3.17)$$

Generally, this equation has two solutions r_1 and r_2 as functions of α, β and γ.

On the other hand, inserting equation (3.14) into equation (3.10) and (3.11), we obtain the characteristic equation for γ,

$$f(\gamma) = (r_2 + \alpha + \gamma) \exp(r_1) - (r_1 + \alpha + \gamma) \exp(r_2) \qquad (3.18)$$

Therefore from this equation, the decay rate of the pdf of the random response time can be solved from the root of this non-linear equation.

3.2 Analytical results and discussion

Given the mean gain <G> and the impact ionization ratio k, the ionization coefficients α and β can be obtained from Eq.(2.3). Therefore r_1 and r_2 can be solved from Equation (3.17) for each value of γ. Then the decay rate γ can be solved from the root of the characteristic equation (3.18). Fig.(3.1) shows the decay rate γ as a function of the impact ionization ratio k, for the fixed mean gain <G>=10, 20 and 40. Figure (3.2) shows the decay rate as a function of mean gain for the several fixed impact ionization ratios, k = 0.2, 0.4, 0.6, 0.8 and 1.0. As shown in Fig. (3.1) and (3.2), for the fixed impact ionization ratio, the decay rate increases as mean gain decreases and decreases as the impact ionization ratio increases for constant mean gain. The behaviour of the decay rate as functions of mean gain and impact ionization ratio is important due to following.

First, the decay rate is critical in calculating the statistics of the mean response time, e.g., the mean response time, variance of the response time, etc., because even if the absolute value of the pdf tail of the random response time is very small, the statistics of the random response time may still be greatly influenced by the decay rate if the decay rate is small. Second, precise numerical calculation of the decay rate is very difficult, especially in the region of the large mean gain and high impact ionization ratio. This is because if

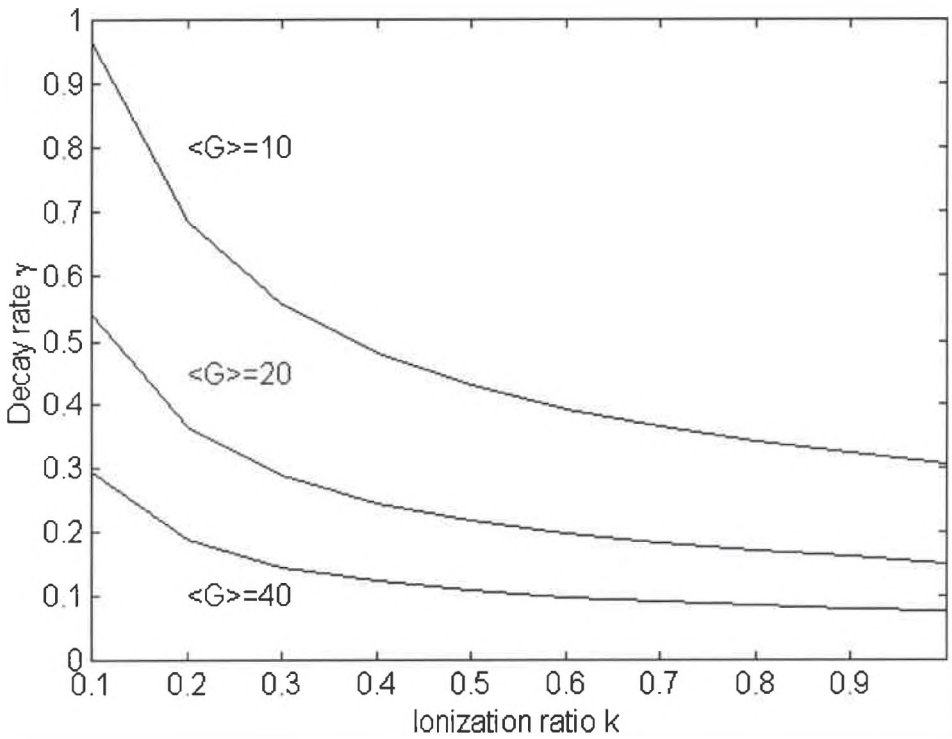

Figure 3.1: Analytical decay rate γ of the pdf of the random response time T as a function of impact ionization coefficient ratio k.

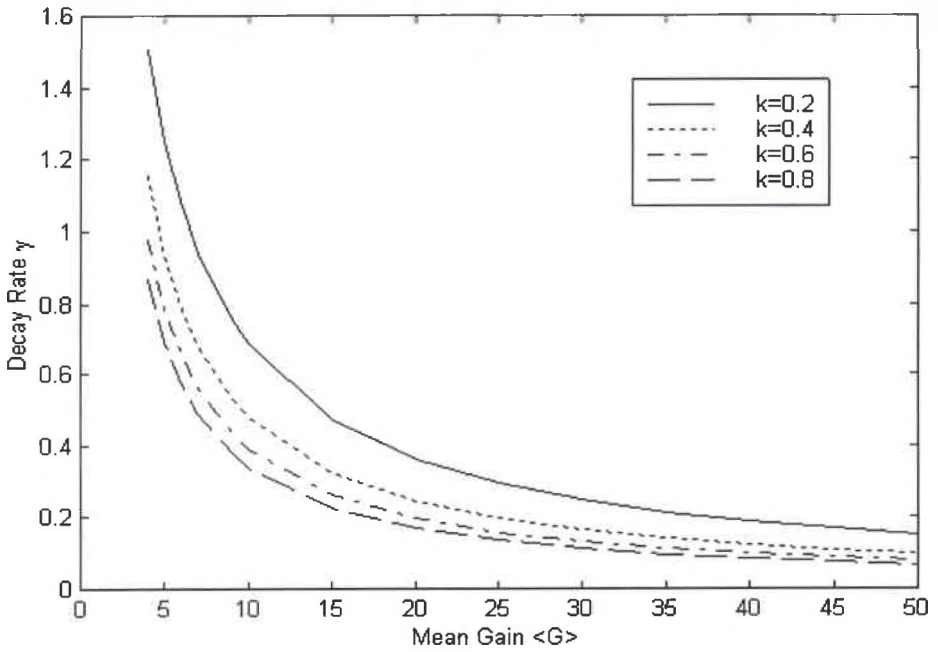

Figure 3.2: Analytical decay rate γ of the pdf of the random response time T as a function of mean gain <G>.

the impact ionization ratio and the mean gain are large, then there are necessary many carrier ionizations involved in the multiplication region. It will take a long time for all the electrons and holes to exit the multiplication region. Therefore, the tail of the pdf of the mean response time will decay at slow rate. An accurate numerical solution will require a large number of iterations.

3.3 Comparison with the numerical results

The approximate analytical results are compared with the numerical results obtained by solving the renewal equations numerically. The comparison results are shown in the Figure (3.3). Which shows the decay rate γ as a function of impact

ionization rate k for fixed mean gain. Numerical results are in good agreement with the approximate analytical results, except the region of large mean gain and high ionization, as expected.

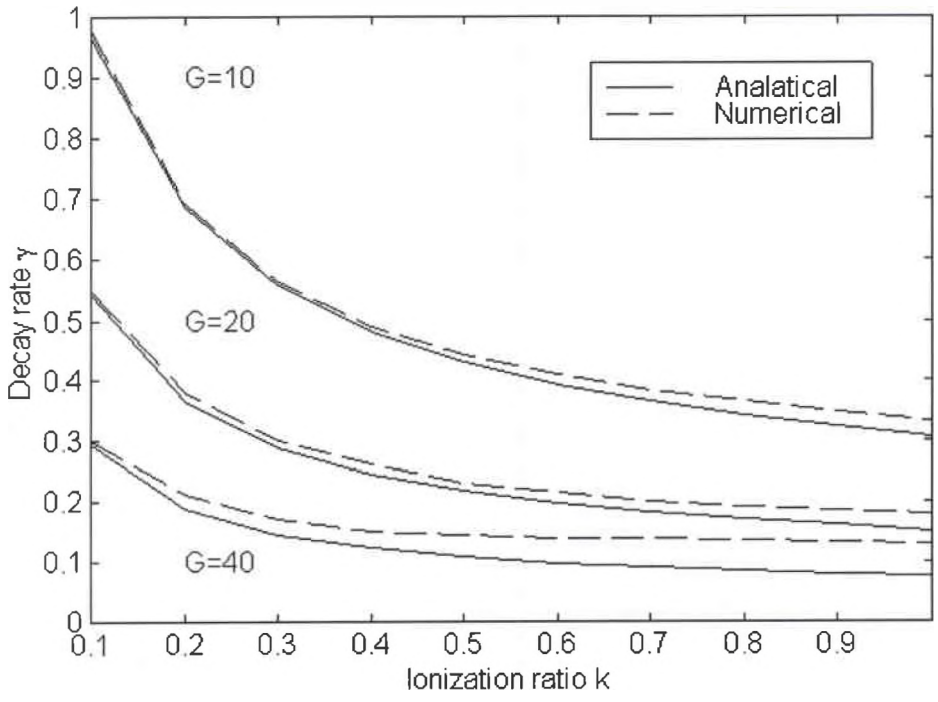

Figure 3.3: Comparison between the numerical and analytical decay rate γ of the probability density function of the random response time T.

As discussed in the Section 3.1, the decay in the density function of T is exponential only when t is large. This condition usually can be met for t excess of 6 times the transition time τ_e for small mean gain.

CHAPTER IV

APPLICATIONS

In the Chapter II, we have derived the renewal equations for the distribution function of APD random response time. Numerical solutions to the renewal equations and a discussion of results were presented. In the chapter III analytical solutions to the decay rate of the pdf of the random response time were obtained. The analytical solutions are important since it gives us the knowledge of the behaviour of the mean response time, and also will help making conclusions on the maximum allowable data rate to keep the effect of intersymbol interference minimal. Most importantly, the method presented in this thesis gives us a simple way to calculate the statistics of the impulse response function to be considered next.

The statistics of the impulse response function, including the mean, standard deviation, and characteristic function (all as functions of time) were previously determined by Hayat [51]. The approach he used is based on the renewal equations for the number of carriers of one kind, (i.e., electron or hole), at time t after the initiation of the multiplication process by a single carrier of a certain kind at an arbitrary location within the multiplication region. Kahram [33] on the other hand, derived the autocorrelation function of the impulse response of a double carrier multiplication APD,

based on a discrete stochastic numerical model. Both methods require extensive computing.

In this chapter, we present a simple approximation to calculate the mean, the standard deviation, and autocorrelation function of the random impulse response. Our method is based on simple impulse response function models and the pdf of the random response time.

4.1 Impulse response function

We assume the random impulse response function as following three simple models. The impulse response function is modelled in terms of random response time T, and electron transition time τ_e.

(1) Rectangular response model

$$H(t) = \frac{G}{T}\mathrm{Re}c\left(\frac{t}{T} - \frac{1}{2}\right) \tag{4.1}$$

This is a simple response model. For which we assume that a constant response during the duration of the random response time T (see Fig.(4.2)).

(2) Triangle response model

$$H(t) = \begin{cases} \dfrac{2G}{\tau_e T} T \\ -\dfrac{2G}{(T-\tau_e)} t + \dfrac{2G}{T-\tau_e} \end{cases} \tag{4.2}$$

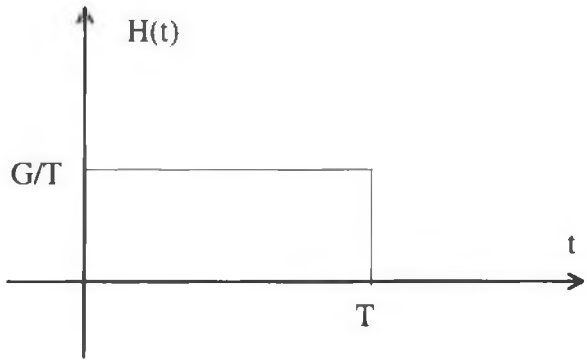

Figure 4.2. Rectangular response model

In this rectangular model, we over emphasis the response at $t>\tau e$. The triangle model is close to the real impulse response function. Of course, we can use more precise random impulse response function model to get more correct results. In this paper, we only use these simple models to get some intuitive results. Some sophisticated models can be adopted only by slightly adjusting the computation.

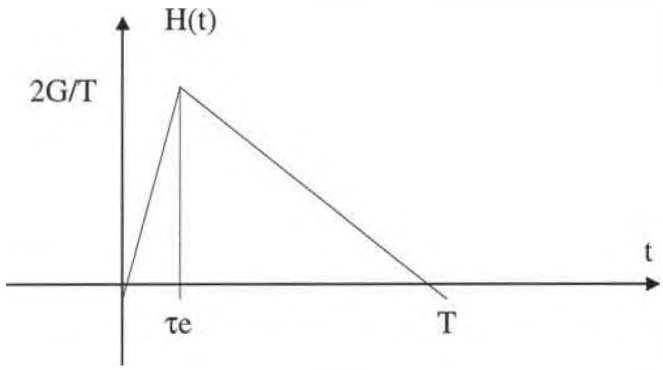

Figure 4.3: Triangle Response Model

4.2 Statistics of the random impulse response function

Based on the pdf of the random response time T and the simple random response models described above, the statistics of the impulse response function can then simply be determined.

Let h(t) be the mean of the random process H(t), i.e., h(t) = E[H(t)], and let Var(H(t)) denote the variance of H(t).

It can be shown that for the rectangle model, the mean and the variance of the H(t) are,

$$h(t) = < G > \int_0^{\infty} \frac{1}{\tau} \mathrm{Re}c\left(\frac{t}{\tau} - \frac{1}{2}\right) f_t(\tau) d\tau$$

$$= < G > \int_t^{\infty} \frac{1}{\tau} f_T(\tau) d\tau \quad = < G > E[\frac{1}{T}] \quad = < G > E[\frac{1}{T}] \tag{4.3}$$

$$E[H^2(t)] = < G >^2 \int_0^{\infty} \frac{1}{\tau^2} f_T(\tau) d\tau \quad = < G >^2 \; E[\frac{1}{T^2}] \tag{4.4}$$

and the variance is,

$$Var[H(t)] = < G >^2 \; E\left[\frac{1}{T^2}\right] - < G >^2 \left(E\left[\frac{1}{T}\right]\right)^2 \tag{4.5}$$

For the triangle response model, the mean is following,

for $0 \le t \le \tau_e$

$$h(t) = \frac{2 < G > t}{\tau_e} \int_0^\infty \frac{1}{\tau} f_T(\tau) d\tau$$

$$= \frac{2 < G > t}{\tau_e} E[\frac{1}{T}]$$

for $\tau_e \leq t \leq \infty$

$$h(t) = 2 < G > \int_t^\infty \left[\frac{-t}{(\tau - \tau_e)} + \frac{1}{\tau - \tau_e} \right] f_T(\tau) d\tau \qquad (4.6)$$

and the variance can be calculated from the second moment of H(t), that is,

$$E[H(t)^2] = \left(\frac{2 < G > t}{\tau_e} \right)^2 E\left[\frac{1}{T^2} \right] \qquad 0 \leq t \leq \tau e$$

$$E[H(t)^2] = (2 < G >)^2 \int_t^\infty \left[\frac{1}{\tau - \tau_e} - \frac{t}{(\tau - \tau_e)\tau} \right]^2 f_T(\tau) d\tau \qquad \tau e \leq t \leq T \qquad (4.7)$$

therefore,

$$Var[H(t)] = \left(\frac{2 < G > t}{\tau_e} \right)^2 \{ E[\frac{1}{T^2}] - E[\frac{1}{t}]^2 \} \qquad \text{for} \quad 0 \leq t \leq \tau e$$

$$Var[H(t)] = (2 < G >)^2 \left\{ \int_t^\infty \left[\frac{1}{\tau - \tau_e} - \frac{t}{(\tau - \tau_e)\tau} \right]^2 f_T(\tau) d\tau - \left[\int_0^\infty \left[\frac{1}{\tau - \tau_e} - \frac{t}{(\tau - \tau_e)\tau} \right] f_T(\tau) d\tau \right]^2 \right\}$$

for $\tau e \leq t \leq T$ (4.8)

4.3 Signal to noise ratio of the impulse response function

Knowledge of the mean and the variance of the detector impulse response function are not sufficient to evaluate the bit-error-rate in a digital optical communication system

[59,60]. Since the response to a random sequence of photons is the sum of the electrical pulses generated by each of the photon. The properties of the photoelectric current are determined not only by the mean and variance of the impulse response function, but also the autocorrelation function.

Once we have computed the variance and the mean of impulse response, the signal to noise

ratio of the current are simple found to be,

$$SNR = \frac{E[H(t)]^2}{Var[H(t)]} \tag{4.11}$$

CHAPTER V

CONCLUSIONS

Renewal equations are developed to calculate the probability distribution function of the random response time of a double-carrier multiplication APD, and used to determine the statistics of the random response time.

The decay rate of pdf of the random response time is a key factor to calculate the statistics of the random response time. We provide in this thesis an analytical approximation to this rate. Our numerical results are in good agreement with the analytical results. The computed statistics of the APD random response time show that the mean response time increases with impact ionization ratio and the mean gain. The variance of the response time increases slowly with the impact ionization ratio for small mean gain, but increase more significantly for high mean gains. Also, from the computed probability density function of the response times, it is found that the decay rate of the density function decreases as the impact ionization ratio and the mean gain increase. Our computation results clearly show the general random response time statistics of different types of APD's.

Although, Si and Ga APD's can be operated at very high gain, in the practical point of view, APD's in communication receivers are usually operated in an optimum

condition to minimize the noise [33]. For the low value of the impact ionization ratio k, (representative of a short-wavelength APD's such as Si APD's), the optimum gain is near 50 for k = 0.01. Whereas for the high value of k, which is more representative of a long wavelength device, the optimum gain is much low, the mean gain is about 10 for k =0.25. From our results, for the low k devices, the mean and variance of the random response time is lower than these of the high k devices. The high variance means that long tail of the random response time. This long tail will degrade the performance of the optical communication systems because of the increasing intersymbol interference. Therefore, APD receivers with high value of k must be operated at the low gain region to get best performance. Otherwise long response time and high response time variance will increase the intersymbol interference, resulting in degrading the system performance. On the other hand, for the APD receivers with low value of k, they can be operated at high gain region. Our results in this thesis generally consistent with the rules of thumb used in optimal receiver design [33,36,60], and can be used as an important guildline in the optical receiver design.

The method provided in this thesis is a general one. It can be easily extended to incorporate the effect of dead space by incorporating the ionization probability, which is a function of position and electric field, into the renewal equations. By using the ionization probability, the nonlocalized ionization processes can also be readily associated to our model.

From the computational point of view, it is important to note that the iteration method is a simple and efficient numerical recipe. The major part involved is just nested

loops. It can simply be implemented in C++. It is efficient, because using a SUN SPARC workstation, the iteration method solves the integral equations of the electron and hole distribution function of the random response time in a average of a couple of dozen iterations within a tolerance of 10e-14. Of course, the algorithm may be improved to increase speed and reduce memory requirement.

REFERENCES

1. B. L. Kasper and J. C. Campbell, "Mutigigabit-per-second avalanche photodiode lightwave receivers," *J. Lightwave Technol.,* vol.LT-5, pp1355-1364, 1987.

2. J. C. Campbell, "Heterojunction photodetectors for optical communications," *Heterostructures and Quantum Devices*, New York: Academic Press, 1994.

3. S. Fujita, N. Henmi, I. Takano, M. Yamaguchi, T. Torikai, T. Suzaki, S. Takano, H. Ishihara, and M. Shikada, "A 10 Gbit/s 80m optical fiber transmission experiment using a directly modulated DFB-LD and a high speed InGaAs APD," *Tech. Dig. OFC'88*, New Orleans, LA, postdeadline paper, 1988.

4. R. G. Smith and S. R. Forrest, "Sensitivity of avalanche photodetector receivers for long wavelength optical communications," *Bell Syst. Tech. J.,* vol.61, pp.2929-2946, 1982.

5. A. R. Hawkins, T. E. Reynolds, D. R. England, D. I. Babic, M. J. Mondry, K. Streubel, and J. E. Bowers, "Silicom hetero-interface photodetector," *Appl. Phys. Lett.*, vol.68, pp.3692-3694,1996.

6. T. P. Pearsall, "Impact ionization rates for electrons and holes in $Ga_{0.47}In_{0.53}As$," *Appl. Phys. Lett.*, vol.36, pp.218-220,1980.

7. L. W. Cook, G. E. Bulman, and G. E. Stillman, "Electron and hole impact ionization coefficients in GaAs," *Solid-State Electron,* vol.21, pp.331-340, 1978.

8. R. J. McIntyre, "Mutiplication noise in uniform avalanche diodes," *IEEE Trans. Electron Dev.,* vol.13, pp.164-168, 1966.

9. L. E. Tarof, J. Yu, R. Bruce, D. G. Knight, T. Baird, and Oosterbrik, "Planer InP/InGaAs avalanche photodetectors with partial charge in the device periphery," *Appl. Phys. Lett.*, vol.57, pp.670-672, 1990.

10. L. E. Tarof, J. Yu, R. Bruce, D. G. Knight, T. Baird, and Oosterbrik, "High frequency performance of separate absorption, grading, charge, and multiplication InP/InGaAs avalanche photodiodes," *TEEE Photon. Technol. Lett.*, vol.5, pp.672-674,1993.

11. J. Yu, L. E. Tarof, R. Bruce, D. G. Knybt, K. Visuanatha, and T. Baird, "Noise performance of separate absorption, grading, charge, and multiplication InP/InGaAs avalanche photodiodes," *TEEE Photon. Technol. Lett.*, vol.6, pp.632-634,1994.

12. M. S. Unlu, and S. J. Strite, "Resonant cavity enhanced photonic devices," *J. Appl. Phys.*, vol.78, no.2, pp.607-639,1995.

13. S. S. Murtaza, R. V. Chelakara, R. D. Dupuis, and J. C. Campbell, "Resonant cavity photodiode operating at 1.55 μm with Burstein-shifted $In_{0.53}Ga_{0.47}As$/iNp reflectors," *Appl. Phys. Lett.*, vol.69, no.17, pp.2462-2464, 1996.

14. S. Y. Chou, and M. Y. Lin, "Nanoscale tera-hertz meatal-semiconductors metal photodetectors," *IEEE J. Quantum Electron.* Vol. 28, no.10, pp.2358-2368, 1992.

15. L. Y. Lin, M. C. Wu, T. Itoh, T. A. Vang, R. E. Muller, D. L. Sivlo, and A. Y. Cho,"Velocity matched distributed photodetectors with high saturation power and large bandwidth," *IEEE Photon Technol. Lett.,* vol.8, no. 10, pp.1376-1378, 1996.

16. C. L. Goldsmith, G. A. Magel, B. M. Kanack, R. J. Baca, "Coherent combining of RF signals in a traving wave photodetector array," *IEEE Photon Technol. Lett.*, vol. 9, no. 7, pp.988-990,1997.

17. Majeed M. Hayat, and Bahaa E. A. Saleh, "Statistical propertiesof the impulse response function of double carrier mutiplication avalanche photodiodes including the effect of dead space," *J. of Lightwave Technol.,* vol.10, no.10, pp.1415-1425,1992.

18. M. C. Teich, K. Matsuo, and B.E. A. Saleh, "Time and frequency response of the conventional avalanche photodiode," *IEEE Trans. Electron. Dev.,* vol.ED-33, pp.1511-1517,1986.

19. J. J. O'Reilly, J. R. F. Darocha, "Improved error probability evaluation methods for direct detection optical communication systems," *IEEE Transaction on Information Theory*, vol. IT-33, no. 6, pp.839-848, 1987.

20. M. M. Hayat, B. E. A. Saleh, and J.A. Gubner, "Bit-error rates for optical receivers using avalanche photodiodes with dead space," *IEEE Trans. Commun.,* vol.43, pp.99-106, 1995.

21. G. Kahraman, B. E. A. Saleh, W. L. Sargeant, and M. C. Teich, "Time and frequency response of avalanche photodiodes with arbitrary structure," *IEEE Trans. Electron. Dev.*, vol.39,pp.553-560, 1992.

22. T. Shiba, E. Ishirnura, K. Takahasi, H. Namizaki, and W. Susaki, "New approach to the frequency response analysis of an InGaAs avalanche photodiode," *J. Lightwave Technol.*, vol.6, pp.1502-1505, 1988.

23. J. N. Hollenhorest, "Frequency response theory for multilayer photodiodes," *J. Lightwave Technol.*, vol.8, pp.531-537,1990.

24. J. C. Campbell, W.S. Holden, G. J. Qua, and A. G. Dentai, "Frequency response of InP/InGaAsP/InGaAs APD's with separate absorption grading and mutiplication regions," *IEEE J. Quantun Electron.*, vol. QE-21, pp.1743-1749,1985.

25. J. C. Campbell, B. C. Johson, G. J. Qua, and W. T. Tsang, "Frequency response of InP/InGaAsP/InGaAs APD's," *J. Lightwave Technol.*, vol. 7, pp.778-784,1989.

26. G. A. Baraff, "Distribution function and ionization rates for hot electrons in semiconductors," *Phys. Rev.*, vol.128, no.6, pp.2507-2517, 1962.

27. Y. Okuto, and C. R. Crowell, "Energy-conservation considerations in the characterization of impact ionization in semiconductors," *Phys. Rev.*, vol. B-6, no.8, pp.3076-3081, 1972.

28. R. J. McIntyre, "Mutiplication noise in uniform avalanche diodes," *IEEE Trans. Electron. Dev.,* vol. ED-13, pp.164-168,1966.

29. R. J. McIntyre, "The distribution of gain in uniformaly multiplying photodiodes:theory," *IEEE Trans. Electron. Dev.,* vol. ED-19, pp.703-713, 1972.

30. J. Conradi, "The distribution of gains in uniformaly mutiply photodiodes: experimental," *IEEE Trans Electron. Dev.*, vol. ED-19, pp.713-718, 1972.

31. P. P. Web, R. J. McIntyre, and J. Conradi, "Prooerties of avalanche photodiodes," *RCA Review*, vol.35, pp.234-278,1974.

32. C. A. Lee, R. L. Batdrof, W. Weigmann, and G. Kaminsky, "Time dependence of avalanche precesses in silicon," *J. Appl. Pyss.*, vol. 38, pp.2787-2797, 1966.

33. S. B. Alexander, *Optical communication receiver design*, SPIE Optical Engineering Press, 1997.

34. S. M. Sze, Photodetectors, *Physics of Semicomductor Devices,* John Wily & Sons, New York, 1981.

35. S. D. Personic, "Statics of a general class of avalanche detectors with application to optical communication," *Bell System. Tech. J.,* vol. 50, pp.3075-3095, 1971.

36. S. D. Personic, "Receiver design for digital fiber optic communication systems, I," *Bell System Tech. J.*, vol.52, pp.843-874, 1973.

37. G. E. Stillman, and C.M. Wolf, Chapter 5, Avalanche photodiodes, In *Semiconductors and semimetals, vol. 12, Infrared Detectors II*, edited by R. K. Willardon and Abert C. Beer, Academic Press, New York, 1997.

38. Federico Capasso, Chapter 1, Physics of Avalanche Photodiodes, In *Semiconductors and Semimetals, vol.22, Lightwave communications Technology, Part D. Photodetectors*, edited by W. T. Tsang, Academic Press, 1985.

39. Y. Okuto and C. R. Crowell, "Ionization coefficients in semiconductors: a nonlocalized property," *Physics Rev.*, B,vol.10, no.10, pp.4284-4296,1974.

40. Hin-Fai Chau and Dimitris Pavlidis, "A physics based fitting and extrapolation method for measured impact ionization coefficients in III-V semiconductors," *J. Appl. Phys.*, vol.72, no.2, pp.531-538,1992.

41. G. E. Bulman, et.al., "Experimental determination of impact ionization coefficients in (100) GaAs," *IEEE Electron Dev. Lett.,* vol. EDL-4, pp.181-182, 1983.

42. N. Tabatabaie, et.al., "Impact ionization coefficient in (111) InP," *Applied Physics Letter*, vol. 46, pp.182-184,1985.

43. J. L. Moll, *Physics of Semiconductors*, McGraw-Hill, New York, 1964.

44. S. M. Sze, Chapter 13, *Photodetectors in physics of semiconductor devices*, John Willy & Sons, New York,1981.

45. B. E. A. Saleh, and M. C. Teich, *Fodamental of Photonics*, New York, Wiley,1991.

46. I. M. Nagv, "Effect of time dependence of multiplication process on avalanche noise," *Solid State Electron.*, vol.16, pp.19-28,1973.

47. A. A. Walma, and R. Hackam, "On the time dependency of the avalanche process in semiconductors," *Solid State Electron.*, vol.18, pp.511-517, 1974.

48. K. Matsuo, M. C. Teich, and B.E.A. Saleh, "Noise properties and time response of the staircase avalanche photodiode," *IEEE Trans. Electron.* Dev., vol.EII-32, pp.2615-2623,1985.

49. K. Matsuo, M. C. Teich, and B.E.A. Saleh, "Threshold energy effect on avalanche breakdowm voltage in semiconductor junction," *Solid State Electron.*, vol. 18, pp.161-168, 1974.

50. M. M. Hayat, W. L. Sargeant, and B. E. A. Saleh, "Effect of dead space on gain and noise on Si and GaAs avalanche photodiodes," *IEEE J. Quantun Electron.*, vol. 28, pp.1360-1365,1992.

51. M. M. Hayat, B. E. A. Saleh, and M.C. Teich, "Effect of dead space on gain and noise of double carrier mutiplication avalanche photodiodes," *IEEE Trans. Electron Dev.*, vol.39, pp.546-552, 1992.

52. B.E. Saleh, M. M. Hayat, and M. C. Teich, "Effect of dead space on the excess noise factor and the response of avalanche photodiodes," *IEEE Trans. Electron. Dev.*, vol.37, pp.1976-1984, 1990.

53. Gokalp Kahraman, B. E. A. Saleh, and M.C. Teich, "Spectral propeties of photocurrent fluctuations in avalanche photodiodes," *J. Lightwave Technol.*, vol.10, no.4, pp.458-468, 1992.

54. K. B. Athreya, and P. E. Ney, *Branching Processes*, Berlin, FRG, Springer, 1972.

55. G. Sankaranarayanan, *Branching Process and its Estimation Theory*, New Delhi, India: Wiley Eastern Limited, 1989.

56. I. N. Kovalenko, N.Yukuznctsov, and V. M. Shurenkov, *Models of Random Processes*, CRC Press, New York, 1996.

57. Sergio N. Torres, *Bit-error-rate for communication systems using twin-photon beams*, M.S. Thesis, University of Dayton, Dec., 1997.

58. D. J. H. Maclean, *Optical line Systems*, John Wiley & Sons, 1996.

59. A. Bandyopalhyay, M. Jamal, L. E. Tarof, and W. Clark, "A simplified approach to time domain modeling of avalanche photodiodes," *IEEE J. Quantun Electron.*, vol.34, no.4,1998.

60. N. Z. Hakim, et.al., "Signal to noise ratio for lightwave systems using avalanche photodiodes," *J. Lightwave Technol.*, vol.9, no.3, pp.318-320, 1991.